

Use of Strain-Range Partitioning for Predicting Time-Dependent, Strain- Controlled Cyclic Lifetimes of Uniaxial Specimens of 2½ Cr-1 Mo Steel, Type 316 Stainless Steel, and Hastelloy X

This document has been reviewed and is determined to be
APPROVED FOR PUBLIC RELEASE.

Name/Title: Leesa Laymance/ORNL TIO
Date: 7/30/2020

C. R. Brinkman
J. P. Strizak
M. K. Booker

~~APPLIED TECHNOLOGY~~

Any further distribution by any other of this document or of the data therein to third parties representing foreign interests, foreign governments, foreign companies and foreign subsidiaries or foreign divisions of U.S. companies should be coordinated with the Director, Division of Reactor Research and Technology, Department of Energy.



OAK RIDGE NATIONAL LABORATORY
OPERATED BY UNION CARBIDE CORPORATION - FOR THE DEPARTMENT OF ENERGY

Who uses this Form: All ERDA contractors except those specifically instructed by their ERDA contract administrator to
use shorter Form ERDA-427.

Printed in the United States of America. Available from
the Department of Energy,
Technical Information Center
P.O. Box 62, Oak Ridge, Tennessee 37830
Price: Printed Copy \$6.00; Microfiche \$3.00

This report was prepared as an account of work sponsored by an agency of the United States Government. Neither the United States Government nor any agency thereof, nor any of their employees, contractors, subcontractors, or their employees, makes any warranty, express or implied, nor assumes any legal liability or responsibility for any third party's use or the results of such use of any information, apparatus, product or process disclosed in this report, nor represents that its use by such third party would not infringe privately owned rights.

c. If box c is checked, at least one copy shall be original ribbon or offset and be completely legible. A clear carbon copy is acceptable as a second reproducible copy.

ORNL-5396
~~Distribution~~
~~Category C-77,~~
~~UC-70h, -k~~

Contract No. W-7405-eng-26

METALS AND CERAMICS DIVISION

HTGR BASE TECHNOLOGY PROGRAM

Gas-Cooled Reactor Structure Materials Studies (189a 01332)

USE OF STRAIN-RANGE PARTITIONING FOR PREDICTING
TIME-DEPENDENT, STRAIN-CONTROLLED CYCLIC
LIFETIMES OF UNIAXIAL SPECIMENS OF
2 1/4 Cr-1 Mo STEEL, TYPE 316
STAINLESS STEEL, AND HASTELLOY X

C. R. Brinkman, J. P. Strizak, and M. K. Booker

Date Published: June 1978

OAK RIDGE NATIONAL LABORATORY
Oak Ridge, Tennessee 37830
operated by
UNION CARBIDE CORPORATION
for the
DEPARTMENT OF ENERGY

CONTENTS

ABSTRACT	1
INTRODUCTION	1
EXPERIMENTAL MATERIALS AND PROCEDURE	3
Annealed 2 1/4 Cr-1 Mo Steel	3
Hastelloy X	4
Type 316 Stainless Steel.	4
Specimen Preparation	4
Test Procedure	5
RESULTS	6
Annealed 2 1/4 Cr-1 Mo Steel.	6
Hastelloy X	22
Type 316 Stainless Steel.	26
DISCUSSION	30
Annealed 2 1/4 Cr-1 Mo Steel.	30
Hastelloy X	33
Type 316 Stainless Steel.	34
CONCLUSIONS	36
ACKNOWLEDGMENTS.	38
REFERENCES	38
APPENDIX A	41
APPENDIX B	59
APPENDIX C	65

USE OF STRAIN-RANGE PARTITIONING FOR PREDICTING
TIME-DEPENDENT, STRAIN-CONTROLLED CYCLIC
LIFETIMES OF UNIAXIAL SPECIMENS OF
2 1/4 Cr-1 Mo STEEL, TYPE 316
STAINLESS STEEL, AND HASTELLOY X

C. R. Brinkman, J. P. Strizak, and M. K. Booker

ABSTRACT

The concept of strain-range partitioning was used to estimate the cyclic life of uniaxial specimens subjected to strain-controlled, fully reversed cycling at constant temperatures within the creep range. Strain-time waveforms consisted of ramp loading with tension, or compression, or both tension and compression hold periods at peak strain. Materials examined included 2 1/4 Cr-1 Mo steel in the annealed condition, solution-annealed Hastelloy X, and solution-annealed, thermally aged, or irradiated type 316 stainless steel. Inelastic strain life relationships were either developed directly from appropriate experimental data or obtained via the ductility normalization concept and used with the interaction damage rule. Generally good agreement between experimental and predicted cyclic lifetimes was found, although a number of uncertainties were identified and discussed. In the case of 2 1/4 Cr-1 Mo steel, extrapolations were performed to indicate the influence of hold periods of up to 100 hr at various strain ranges.

INTRODUCTION

Operational cycles of advanced nuclear reactor power generating systems include power adjustments, response to emergency or hypothetical accident situations, and refueling. This mode of operation will subject structural material components to cyclic strain-controlled loading conditions at

elevated temperatures such that the possibility of time-dependent fatigue and creep damage must be considered in their design. Typically, these cycles produce strain ranges that are small, normally being less than about 0.5% with hold periods that are projected to range from as low as perhaps 10 to as high as 1000 hr and with design lifetimes of 30 or 40 years. Accordingly, appropriate elevated-temperature, strain-controlled fatigue data must be generated in the laboratory and methods developed which will allow extrapolation to conditions anticipated in actual service.

It was the objective of this paper to apply concepts of strain-range partitioning to predict the strain-controlled, time-dependent fatigue behavior of several structural materials projected for use in the High-Temperature Gas-Cooled Reactor (HTGR), the Fast Breeder Reactor (FBR), and the Brayton Isotope Power System (BIPS). Comparisons were made between predictions and data generated under isothermal and uniaxial loading conditions for annealed 2 1/4 Cr-1 Mo steel (482-538°C), type 316 stainless steel (593°C) in both the irradiated and unirradiated conditions, and solution-annealed Hastelloy X (871 and 704°C). In the case of 2 1/4 Cr-1 Mo steel, extrapolations of cyclic peak and relaxed stress ranges were performed by several different methods in order to predict the shape of hysteresis loops resulting from both high and low strain-range loading conditions such that the inelastic strain ranges necessary for use in the method of strain-range partitioning could be estimated. These values were then employed to develop fatigue life reduction factors as a function of hold time for several different isostrain-range loading conditions.

The effort presented herein represents an interim report of ongoing test activity and an evaluation of several different methods for extrapolating and correlating uniaxial time-dependent fatigue data.

EXPERIMENTAL MATERIALS AND PROCEDURE

Annealed 2 1/4 Cr-1 Mo Steel

Material used in generating much of the data reported herein was taken from commercial heats of 2 1/4 Cr-1 Mo steel. This consisted of 25-mm-thick (1-in.) plate obtained from Babcock and Wilcox Company, heats 20017 and 3P5601. Chemical analyses of representative material from the plates are compared in Table 1; the other data are in Table 2.

Table 1. Chemical Composition of Alloys

Alloy	Heat	Analysis	Content, Wt %											
			Fe	C	Mn	Si	Cr	Mo	Ni	S	P	N	Co	B
2 1/4 Cr-1 Mo	20017	Vendor	Bal	0.11	0.55	0.29	2.13	0.90		0.014	0.012	0.012		
		ORNL	Bal	0.135	0.57	0.37	2.2	0.92	0.16	0.016	0.012			
Hastelloy X ^a	3P5601	Vendor	Bal	0.12	0.35	0.27	2.3	0.96	0.20	0.022	0.009	0.013		
Type 316 SS ^b	2600-3-4936	Vendor	19.09	0.07	0.58	0.44	21.82	9.42	Bal	<0.005	0.016		1.68	<0.002
	B65808	Vendor	Bal	0.06	1.72	0.40	17.30	2.33	13.30	0.007	0.012		0.030	0.0005

^aAlso 0.63 W.^bAlso 0.065 Cu, 0.003 Ti, 0.0014 Pb, 0.013 Sn, 0.012 Al.

Table 2. Product Form and Grain Size of Alloys

Alloy	Heat	Product Form	Specification	Grain Size		
				ASTM	(mm)	
2 1/4 Cr-1 Mo	20017	Plate	ASME SA-387 Grade D	4-5	55-80	
		Plate	ASME SA-387 Grade D	5	55	
Hastelloy X		13-mm (1/2-in.) Plate	ASME SB-435 (NO 6002)	4	78	
Type 316 SS		Rod		4	80	

Sections of the plates were heat-treated according to the following schedule, which is referred to as an isothermal anneal:

Austenitize at $927 \pm 14^{\circ}\text{C}$ for 1 hr, cool to $704 \pm 14^{\circ}\text{C}$ at a maximum cooling rate of $83^{\circ}\text{C}/\text{hr}$, hold at $704 \pm 14^{\circ}\text{C}$ for 2 hr, and cool to room temperature at a rate not to exceed $6^{\circ}\text{C}/\text{min}$.

Examination of the microstructure of the plate material indicated that the steel contained proeutectoid ferrite, fine pearlite, and some bainite.

Hastelloy X

Specific details concerning the product form, heat number, grain size, and chemical composition of the Hastelloy X are given in Tables 1 and 2.

Type 316 Stainless Steel

Type 316 stainless steel referred to in this investigation came from heat B65808. Specific details are given in Tables 1 and 2.

Specimen Preparation

Following heat treatment, as given above, specimen blanks of either 2 1/4 Cr-1 Mo steel or Hastelloy X were cut from the plate material. Blanks were generally prepared such that their longitudinal axes were parallel to the plate rolling direction. Fatigue specimens had an hourglass-shaped gage section configuration with a radius-to-diameter ratio (R/D) of 6. The minimum diameter of the fatigue specimens was either 6.35 mm (0.25 in.) or 5.08 mm (0.2 in.).

In the case of type 316 stainless steel, all the data were taken from the open literature¹⁻³ and no new tests were

the performed. Data were available from tests that had been conducted on type 316 stainless steel in three conditions:

<u>Condition</u>	<u>Treatment</u>
Solution annealed	Solution annealed 1/2 hr at 1075°C followed by a helium quench
Aged	Aged 3096 or 5040 hr at 593°C in helium-filled capsules or aged 1000 hr at 565°C
Irradiated	Irradiated in helium-filled capsules in Experimental Breeder Reactor II to a fluence of $1-2.63 \times 10^{26} \text{ n/m}^2$ ($E > 0.1 \text{ MeV}$). The irradiation temperature was 580 to 610°C

Test Procedure

Fully reversed axial push-pull testing was accomplished in closed-loop electro-hydraulic fatigue test machines. Axial strain control was maintained by employing a diametral extensometer and a simple diametral-to-axial strain computer. Total strain range, $\Delta\epsilon_t$, was thus determined by the relation

$$\Delta\epsilon_t = (\Delta\sigma/E)(1 - 2\nu) - 2\Delta\epsilon_d, \quad (1)$$

where E is Young's modulus, ν is Poisson's ratio, $\Delta\epsilon_d$ is the diametral strain range, and $\Delta\sigma$ is the peak-to-peak stress range from the hysteresis loops. Heating of the specimens was accomplished by induction, and all testing was accomplished in air. Additional details of test procedure can be found elsewhere.⁴

In addition to the continuous-cycling and strain hold-time tests which were generally conducted at a ramp strain rate of $4 \times 10^{-3}/\text{s}$, a number of cyclic creep tests were conducted to verify some of the basic strain-range life relationships for

annealed 2 1/4 Cr-1 Mo steel.⁵ These tests were conducted in air at 538°C and used a bumpless transfer computer system, which kept the test in strain control for a given cycle except during the hold period, when the test was in load control. Switching from strain control to load control occurred at the onset of the hold period, when a predetermined load was achieved, while switching from load control to strain control occurred at the end of the cycle hold period when a predetermined strain level was obtained. Creep deformation thus occurred each cycle and showed a general acceleration in creep rate as the cycles were continued toward specimen failure.

A complete summary of test data obtained to date for 2 1/4 Cr-1 Mo steel is given in Appendix A.

RESULTS

Annealed 2 1/4 Cr-1 Mo Steel

Results of the cyclic creep tests on annealed 2 1/4 Cr-1 Mo steel are given in Table 3. A visual comparison of the cyclic creep curves generated for heat 3P5601 at the same stress level for two specimens tested with either tension or compressive creep hold periods indicated similar creep rates in tension and compression. However, for heat 20017, a tendency for higher creep rates in tension than in compression was observed. Compressive cyclic creep rates of heats 3P5601 and 20017 were similar for equivalent stress holds. Representative cyclic creep curves are given in Appendix B.

Results of the cyclic creep tests given in Table 3 and strain-controlled relaxation tests^{6,7} were combined with the results of Manson et al.⁵ to form the life relationship lines via the interation damage rule given by

$$\frac{1}{N_{pred}} = \frac{F_{pp}}{N_{pp}} + \frac{F_{pc}}{N_{pc}} + \frac{F_{cp}}{N_{cp}} + \frac{F_{cc}}{N_{cc}} , \quad (2)$$

where

N_{pred} = predicted cyclic life,

$$F_{cp} = \Delta\epsilon_{cp}/\Delta\epsilon_{in},$$

$$F_{pp} = \Delta\epsilon_{pp}/\Delta\epsilon_{in},$$

$$F_{pc} = \Delta\epsilon_{pc}/\Delta\epsilon_{in},$$

$$F_{cc} = \Delta\epsilon_{cc}/\Delta\epsilon_{in}.$$

$\Delta\epsilon_{in}$ is the total inelastic strain range, while the inelastic strain components are defined as follows:

$\Delta\epsilon_{pp}$ = tensile plastic strain reversed by compressive plastic strain,

$\Delta\epsilon_{pc}$ = tensile plastic strain reversed by compressive creep strain,

$\Delta\epsilon_{cp}$ = tensile creep strain reversed by compressive plastic strain,

$\Delta\epsilon_{cc}$ = tensile creep strain reversed by compressive creep strain.

Table 3. Summary of Cyclic Creep Data for 2 1/4 Cr-1 Mo Steel Generated at 538°C

Specimen	Heat	Total Strain Range (%)	Stress Hold, MPa		Inelastic Strain Components, %					Observed Cycles to Failure, N_{obs}	Time to Failure, t_f (hr)	Stress Amplitude, MPa		β^b	
			Tensile	Compressive	$\Delta\epsilon_{in}^a$	$\Delta\epsilon_{pc}$	$\Delta\epsilon_{cp}$	$\Delta\epsilon_{cc}$	$\Delta\epsilon_{pp}$			Tensile	Compressive		
ITL-62	3P5601	2.98	248	248	2.66	2.33			0.33	293	274	319.	248	0.93	
I606T	20017	2.97	248	248	2.65	2.25			0.40	320	133	312	248	0.90	
ITT-11	3P5601	2.00	243	243	1.69	1.18			0.51	496	227	288	243	0.83	
I6009	20017	2.00	243	243	1.69	1.42			0.27	509	202	305	243	0.91	
ITT-18	3P5601	1.00	243	243	0.72	0.31			0.41	1,386	15.4	252	243	0.68	
I6006	20017	1.00	243	243	0.72	0.37			0.35	1,252	29.3	248	243	0.75	
ITF12	3P5601	0.71	226	226	0.44	0.16			0.28	2,758	47.7	233	226	0.61	
I6016	20017	0.71	226	226	0.43	0.24			0.19	2,345	58.3	250	226	0.78	
ITT-17	3P5601	0.56	207	207	0.32	0.13			0.19	2,593	59.0	221	207	0.86	
I607T	20017	0.56	209	209	0.31	0.14			0.17	3,248	231	209	209	0.85	
ITT-20	3P5601	2.98	253	253	2.63	2.11			0.53	147	136	253	346	0.94	
I602T	20017	2.97	250	250	2.62	2.48			0.14	158	231	230	364	0.98	
ITL-61	3P5601	2.00	241	241	1.69	1.30			0.39	532	172	241	303	0.56	
I604T	20017	2.00	241	241	1.69	1.34			0.35	460	50.2	241	300	0.89	
I608T	20017	2.00	246	246	1.68	1.42			0.26	313	64.6	246	309	0.94	
ITL-100	3P5601	1.02	241	241	0.73	0.28			0.45	1,480	7.6	241	271	0.62	
I603T	20017	1.02	241	241	0.71	0.44			0.28	1,264	38.3	241	286	0.81	
ITL-19	3P5601	0.72	217	217	0.46	0.14			0.32	4,376	217	217	240	0.29	
I6018	20017	0.72	222	222	0.43	0.31			0.12	2,473	222	222	276	0.86	
ITL-22	3P5601	2.96	252	245	2.68	0.16	1.72	0.80	315	240	252	245	0.67		
I609T	20017	2.00	209	210	1.77	0.05	1.08	0.64	534	120	209	210	0.69		
ITL-79	3P5601	1.01	234	228	0.74	0.06	0.28	0.40	1,527	36.6	234	228	0.44		
R6007	20017	1.00	224	224	0.75	0.04	0.32	0.39	1,508	79.2	224	224	0.52		
ITL-68	3P5601	0.70	214	207	0.46		0.01	0.13	0.32	2,974	50.6	214	207	0.47	

^aCalculated using a Young's Modulus value of 174 GPa. The ramp strain rate was 4×10^{-3} /s.

^bDamage factor, $F_{pc} \times N_{obs}/N_{pc}$, $F_{cp} \times N_{obs}/N_{cp}$, or $F_{cc} \times N_{obs}/N_{cc}$. Values should be greater than 0.5 in order to establish life relationship.

Here "plastic" strain is defined at time-independent inelastic strain, while "creep" strain is defined as time-dependent inelastic strain. Equations for the life relationship lines thus obtained were as follows:

$$N_{cp} = 255\Delta\varepsilon_{in}^{-1.777}, \quad (3)$$

$$N_{cc} = 450\Delta\varepsilon_{in}^{-1.24}, \quad (4)$$

$$N_{pc} = 386\Delta\varepsilon_{in}^{-1.07}, \quad (5)$$

$$N_{pp} = 521\Delta\varepsilon_{in}^{-2.67}, \Delta\varepsilon_{in} \leq 0.45\%, \quad (6)$$

$$N_{pp} = 1648\Delta\varepsilon_{in}^{-1.24}, \Delta\varepsilon_{in} \geq 0.45\%, \quad (7)$$

where $\Delta\varepsilon_{in}$ values are measured in percent. It should be noted that in formulating the best-fit life relationship lines expressed by Eqs. (4) through (7), all cyclic creep and relaxation data were employed, even though the particular damage strain fraction⁸ for a given test, e.g., $\emptyset = (F_{cc})(N_{obs}/N_{cc}) > 0.5$ for a "cc" cycle, was not obeyed. In the case of the strain-controlled relaxation tests, particularly those conducted at low total strain ranges, which was our particular interest, the most dominant inelastic strain range was always $\Delta\varepsilon_{pp}$. However, it was thought appropriate to include the strain-controlled data in these formulations, since our purpose was to generate guideline relationships appropriate for design conditions referred to in the introductory section of this paper.

Equations (6) and (7) indicate that in the case of the $N_{pp} = f(\Delta\varepsilon_{in})$ relationship expressed in log-log coordinates, a bilinear relationship was most appropriate (see Fig. 1). Reasons for the break in the otherwise linear relationship on log-log coordinates have been discussed elsewhere.⁷ A comparison of the formulations given in Eqs. (3) through (7) with the appropriate formulations for this material as originally proposed by Manson et al.⁵ generally showed good agreement

(see Fig. 2). A comparison of the various life relationships is given in Fig. 3.

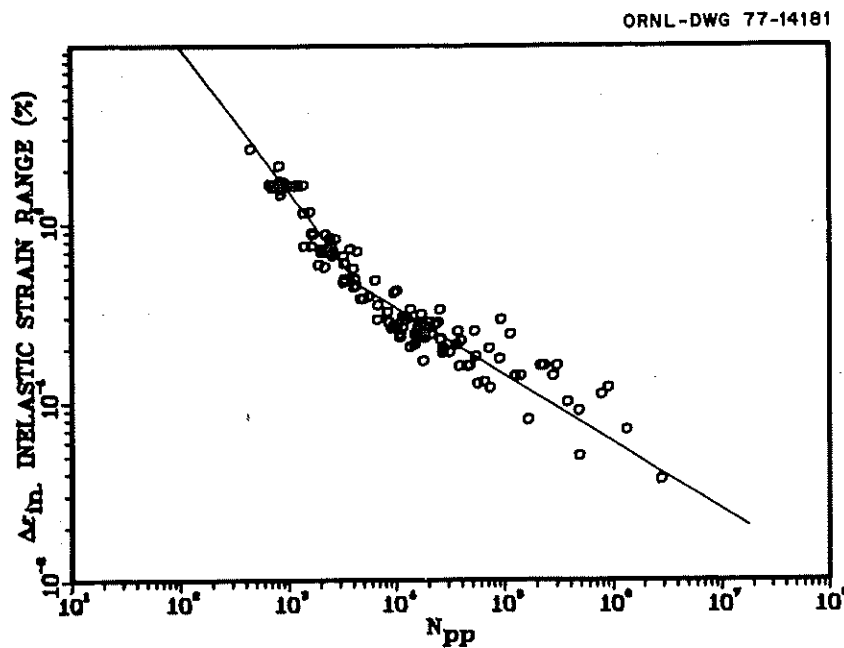


Fig. 1. Strain-Range Partitioning Life Relationship Line for "pp" Strain for 2 1/4 Cr-1 Mo Steel.

Unlike comparisons between cyclic relaxation and cyclic creep data made with the other life relationship line, Fig. 2c also shows that the results of the strain-controlled or cyclic relaxation tests fell somewhat below those of the cyclic creep tests. Therefore, as of this writing, it remains an open question as to whether or not the results obtained to date represent normal scatter or, indeed, that an additional formulation is required to best characterize the strain-controlled "cc" type of loading. Figure 3 shows two possible formulations, one for the strain controlled tests or "cc(r)" and the other for load control or "cc" loading. However, the data are limited and therefore no attempt at separation was made in making predictions [i.e., Eq. (4) was used in all calculations].

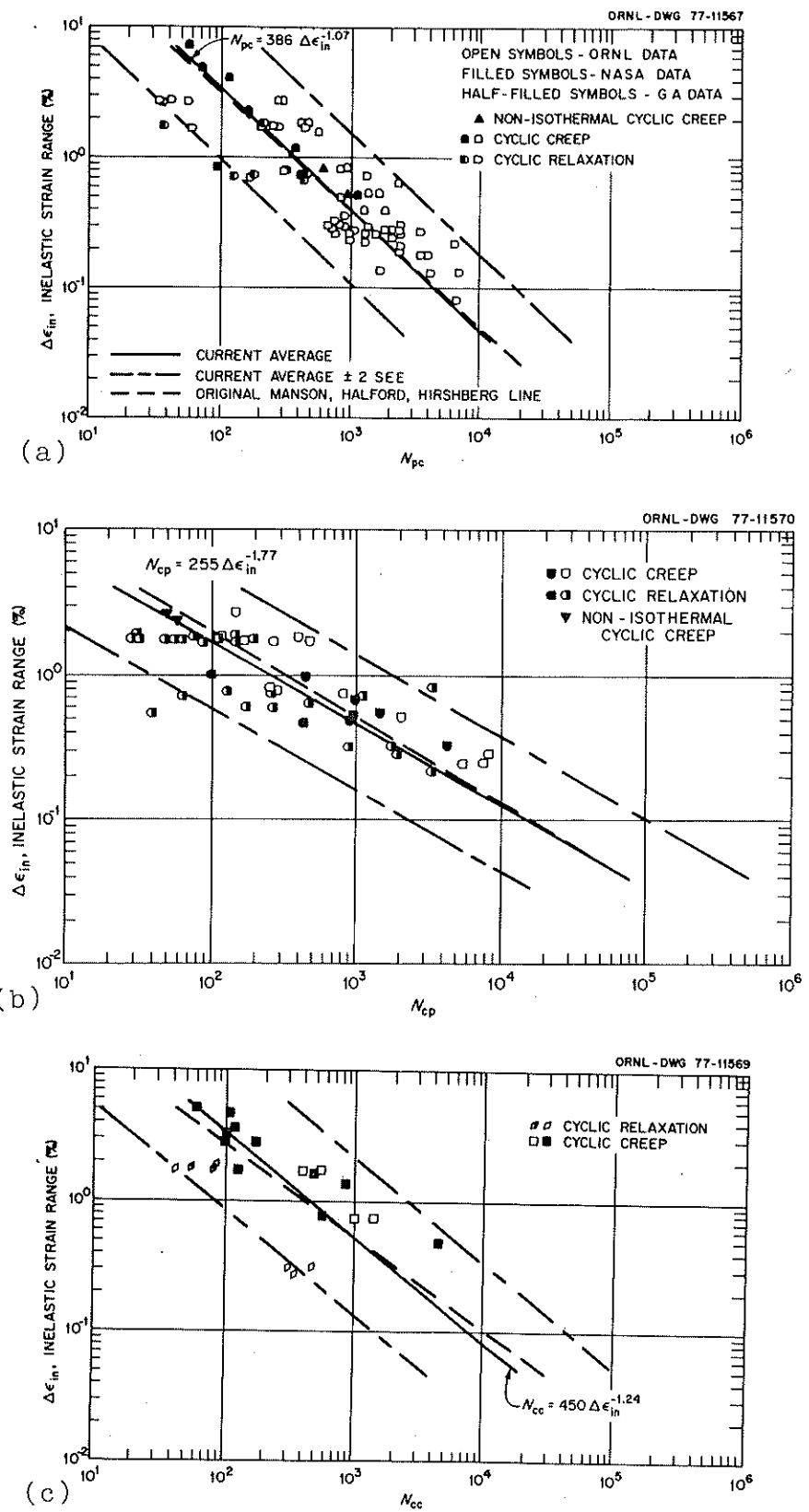


Fig. 2. Strain-Range Partitioning Life Relationships for 2 1/4 Cr-1 Mo Steel.

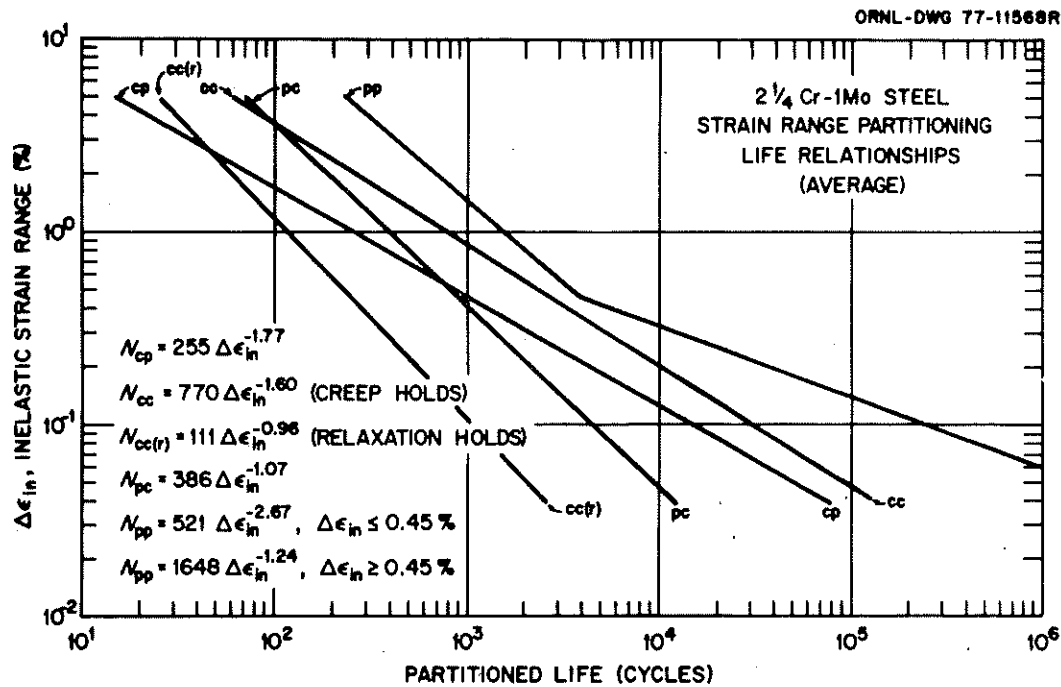


Fig. 3. Comparison of Various Strain-Range Partitioning Life Relationship Lines for 2 1/4 Cr-1 Mo Steel.

With the life relationships, i.e. Eqs. (3)-(7), thus established, the objective was to develop, for fully reversed loading, estimates of the reduction in cyclic lifetimes due to increasing hold periods (times) in strain-controlled situations over the temperature range 482 to 538°C. This estimation can be accomplished via the method of strain-range partitioning if satisfactory approximations of the hysteresis loops appropriate for a given strain range and hold time can be made. Figure 4 shows an example of the changes in hysteresis loops that normally occur for a given strain range and with increasing tensile-only hold times at elevated temperatures. If one can estimate or measure the appropriate steady state or stabilized stress ranges $\Delta\sigma_1, \Delta\sigma_2, \dots, \Delta\sigma_i$, and associated total amount of stress relaxation, i.e., $\Delta\sigma_{r1}, \Delta\sigma_{r2}, \dots, \Delta\sigma_{ri}$, for increasing hold periods t_1, t_2, \dots, t_i , then the key features of the proposed hysteresis loops and associated inelastic strain ranges can be calculated.

ORNL-DWG 77-20490

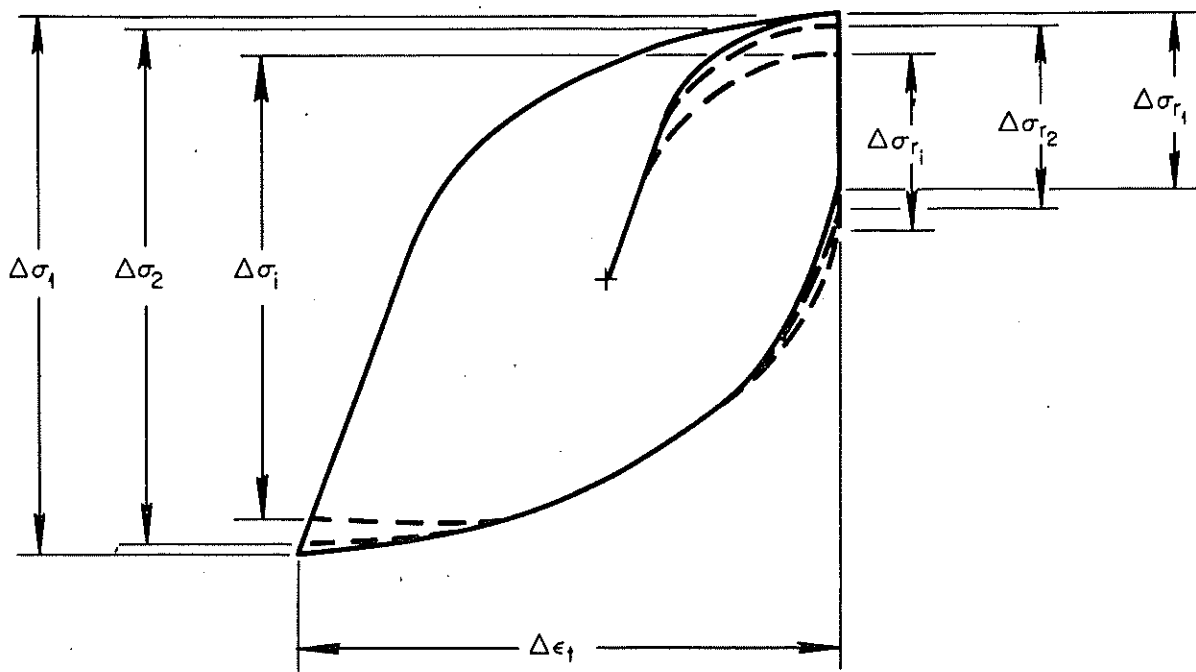


Fig. 4. Schematic Diagram of Typical Strain-Controlled Hysteresis Loop Showing Changes in Stabilized Stress Ranges That Occur at a Constant Strain Range with Increasing Hold Time.

The first step taken was to estimate total stress ranges ($\Delta\sigma$) associated with particular hold periods, strain ranges, and temperatures. This was accomplished using the available data base and extrapolating graphically on semilogarithmic coordinates, stress range vs time (see Fig. 5). It was also found that log-log coordinates could be used. Estimates of the relaxed stress amplitude (σ) from the peak stress amplitude ($\sigma_0 = \Delta\sigma/2$) can be made in a number of ways as follows:

1. employing the Gittus relaxation equation

$$\ln(\sigma_0/\sigma) = Ct^m \quad (8)$$

where C and m are constants for a given strain range and

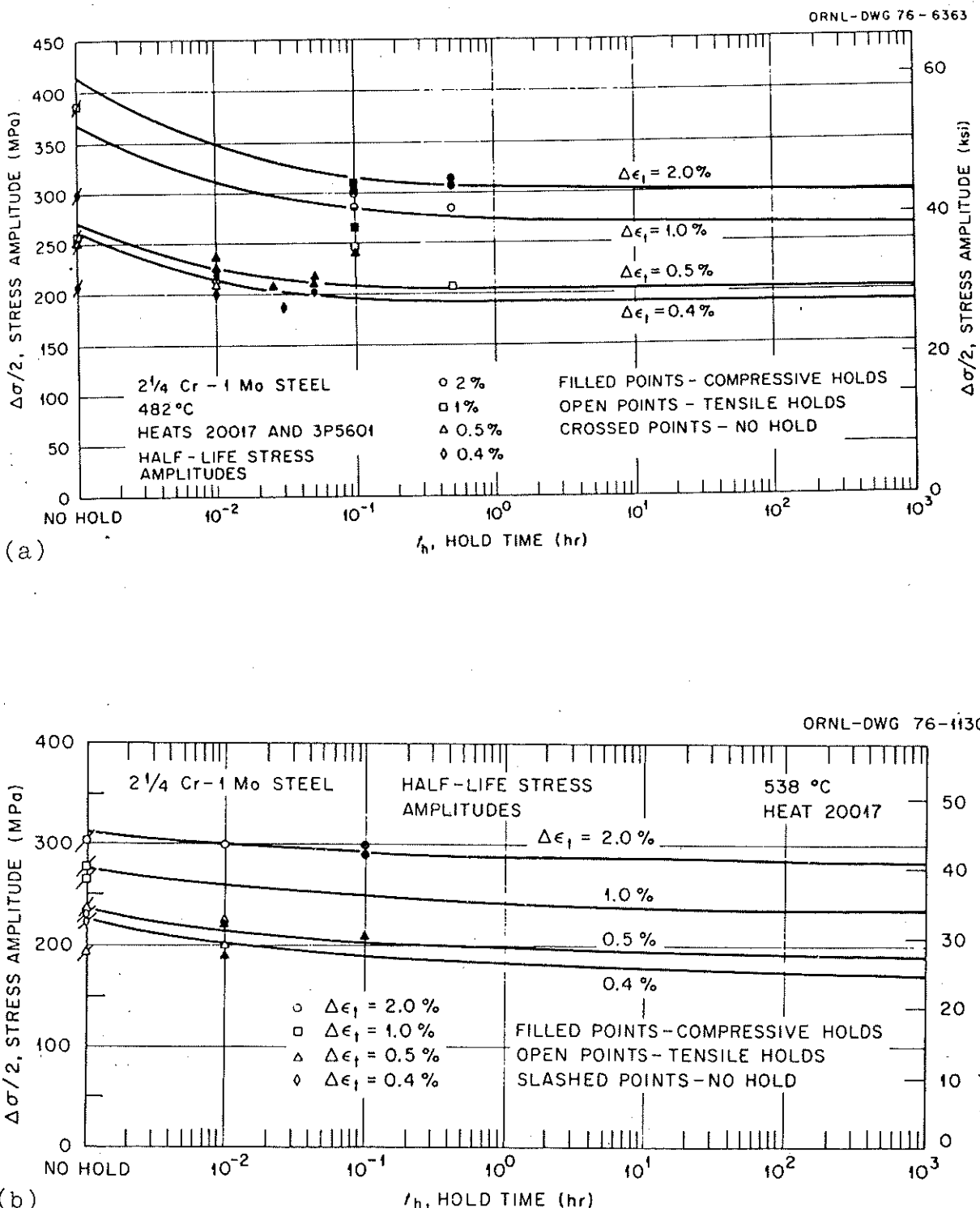


Fig. 5. Variation of Half-Life Stress Amplitude with Hold Time for 2 1/4 Cr-1 Mo Steel at 538°C.

- temperature and are determined experimentally, and t is the required time for relaxation from σ_0 to σ ;
2. using an appropriate creep equation to predict relaxation behavior;⁹
 3. using isochronous cyclic stress relaxation curves for the material involved;
 4. graphical extrapolation from known values of σ_0 .

In case of estimating the time-dependent fatigue behavior of 2 1/4 Cr-1 Mo steel, only the first two methods were employed.

Hypothetical hysteresis loop inelastic time-dependent and -independent strain-range values were then calculated using the following equations (assuming zero means stress):

1. Compressive or Tensile-Only Hold Periods

$$\Delta\epsilon_t = \Delta\epsilon_{in} + \Delta\epsilon_e , \quad (9)$$

$$\Delta\epsilon_{in} = \Delta\epsilon_{pc} \text{ or } \Delta\epsilon_{cp} + \Delta\epsilon_{pp} , \quad (10)$$

$$\Delta\epsilon_{in} = \Delta\epsilon_t - (\Delta\sigma - \Delta\sigma_r)/E , \quad (11)$$

$$\Delta\epsilon_{in} = \Delta\epsilon_t - (\sigma_0 + \sigma)/E , \quad (12)$$

$$\Delta\epsilon_{pc} \text{ or } \Delta\epsilon_{cp} = \Delta\sigma_r/E = (\sigma_0 - \sigma)/E , \quad (13)$$

where $\Delta\epsilon_t$, $\Delta\epsilon_{in}$, $\Delta\epsilon_e$ are the total, inelastic, and elastic strain ranges, respectively, and E is Young's modulus.

2. Compressive and Tensile Hold Periods of Equal Duration

$$\Delta\epsilon_{in} = \Delta\epsilon_{pp} + \Delta\epsilon_{cc} , \quad (14)$$

$$\Delta\epsilon_{in} = \Delta\epsilon_t - (\Delta\sigma - 2\Delta\sigma_r)/E = \Delta\epsilon_t - 2\sigma/E , \quad (15)$$

$$\Delta\epsilon_{cc} = \Delta\sigma_r/E = (\sigma_0 - \sigma)/E . \quad (16)$$

Estimating the relaxed stress range, $\Delta\sigma_r$, and hence the inelastic strain components in the above manner obviously introduces some uncertainty. Accordingly, estimated $\Delta\sigma_r$

values were multiplied by an arbitrary factor of 1.2 as a first approximation to the possible uncertainty and in an effort to see the impact of this variation at various strain ranges and modes of damage, e.g., "pc," "cp," and "cc." Results of all numerical calculations are given in Appendix C.

Figures 6 and 7 then show predictions of the influence of increasing the duration of compressive hold times to 100 hr, imposed each cycle on the hold-time reduction factor, N_f^o/N_h , at a temperature of 482°C. The hold-time reduction factor is simply defined for a given strain range as the cycle life, N_f^o , of a continuously cycled specimen for which the strain rate was $4 \times 10^{-3}/\text{s}$ divided by the estimated cycle life, N_h , for the indicated hold time. Figure 6 shows estimates for a single strain range, i.e., 0.4%, and for the two heats of 2 1/4 Cr-1 Mo steel under investigation. Two bands, shown by the slashed lines, the width of which is defined by 1.2 or $1.0\Delta\sigma_r$, are shown, since these heats, i.e., 3P5601 and 20017, characteristically show different high cycle fatigue endurance levels at this temperature and strain range. Also shown for comparison purposes are results of actual strain-controlled fatigue tests conducted with the indicated compressive hold periods. Estimates of the amount of stress relaxation, $\Delta\sigma_r$, projected for the stabilized hypothetical hysteresis loops were achieved by using the Gittus equation to establish the relaxed stress amplitude (σ). The required Gittus equation constants were obtained from an analysis of some of the experimental data shown in these figures. Also shown by the dashed line is an estimate of the approximate duration of hold period required to cause failure in 250,000 hr at that strain range, e.g., (35 hr hold per cycle) (289, 868 cycles or continuous cycle life)/(40 hold-time reduction factor for 35 hr hold) = 253,634 hr.

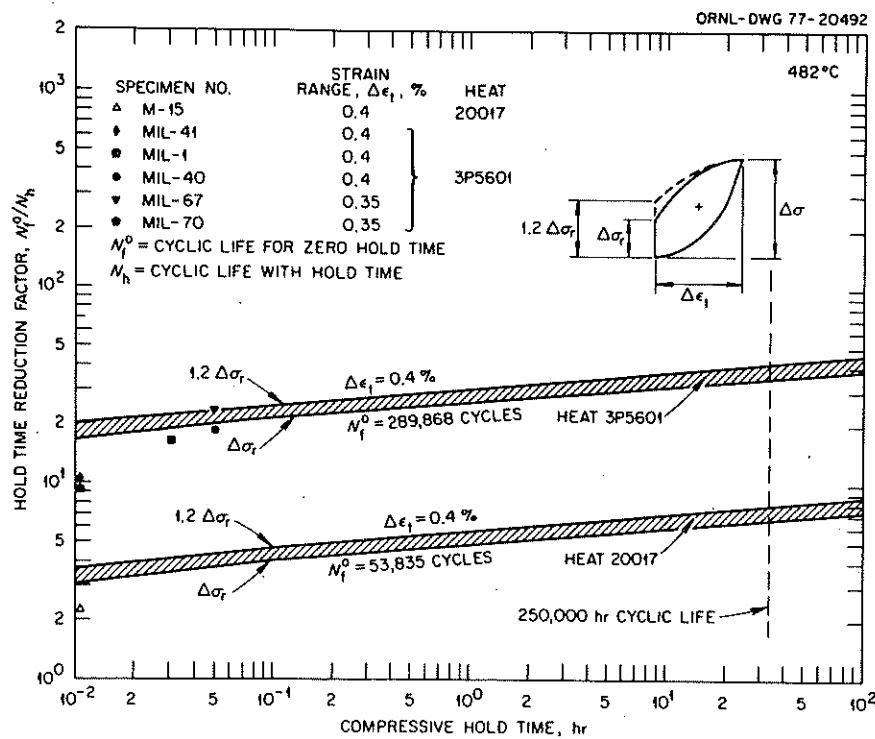


Fig. 6. Comparison of Measured and Predicted Hold-Time Reduction Factors for 2 1/4 Cr-1 Mo Steel and Subjected to Compressive Hold Times at 482°C.

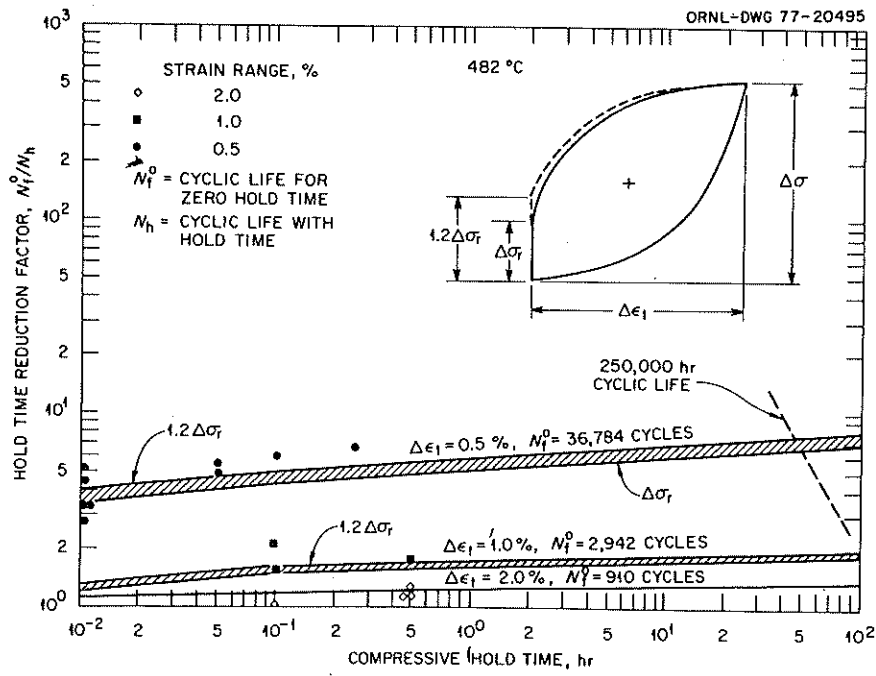


Fig. 7. Comparison of Measured and Predicted Hold-Time Reduction Factors for 2 1/4 Cr-1 Mo Steel Subjected to Compressive Hold Times at 482°C.

Figure 7 shows additional comparisons between experimental results from both heats of 2 1/4 Cr-1 Mo steel for compressive hold times and predicted estimates for total strain ranges of 2, 1.0, and 0.5%. No distinction between heats is made in Fig. 7 since similar behavior was indicated at these strain ranges. Characteristically, the width of the estimated predictive band increases with decreasing strain range. Both Figs. 6 and 7 show good agreement between estimated and actual hold-time reduction factors.

Figures 8 and 9 show similar results for behavior at 482°C for various strain ranges involving tensile and both tensile and compressive hold times respectively. In Fig. 6 the arrows associated with several of the data points indicate where failure would be predicted to occur from a knowledge of the stabilized hysteresis loop for that particular test.

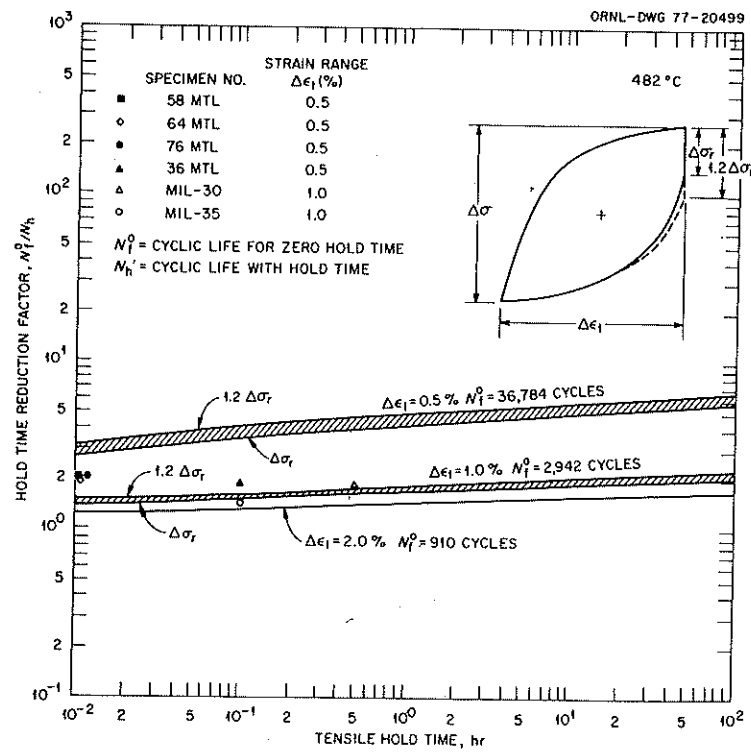


Fig. 8. Comparison of Measured and Predicted Hold-Time Reduction Factors for 2 1/4 Cr-1 Mo Steel Subjected to Hold Tensile Times at 482°C.

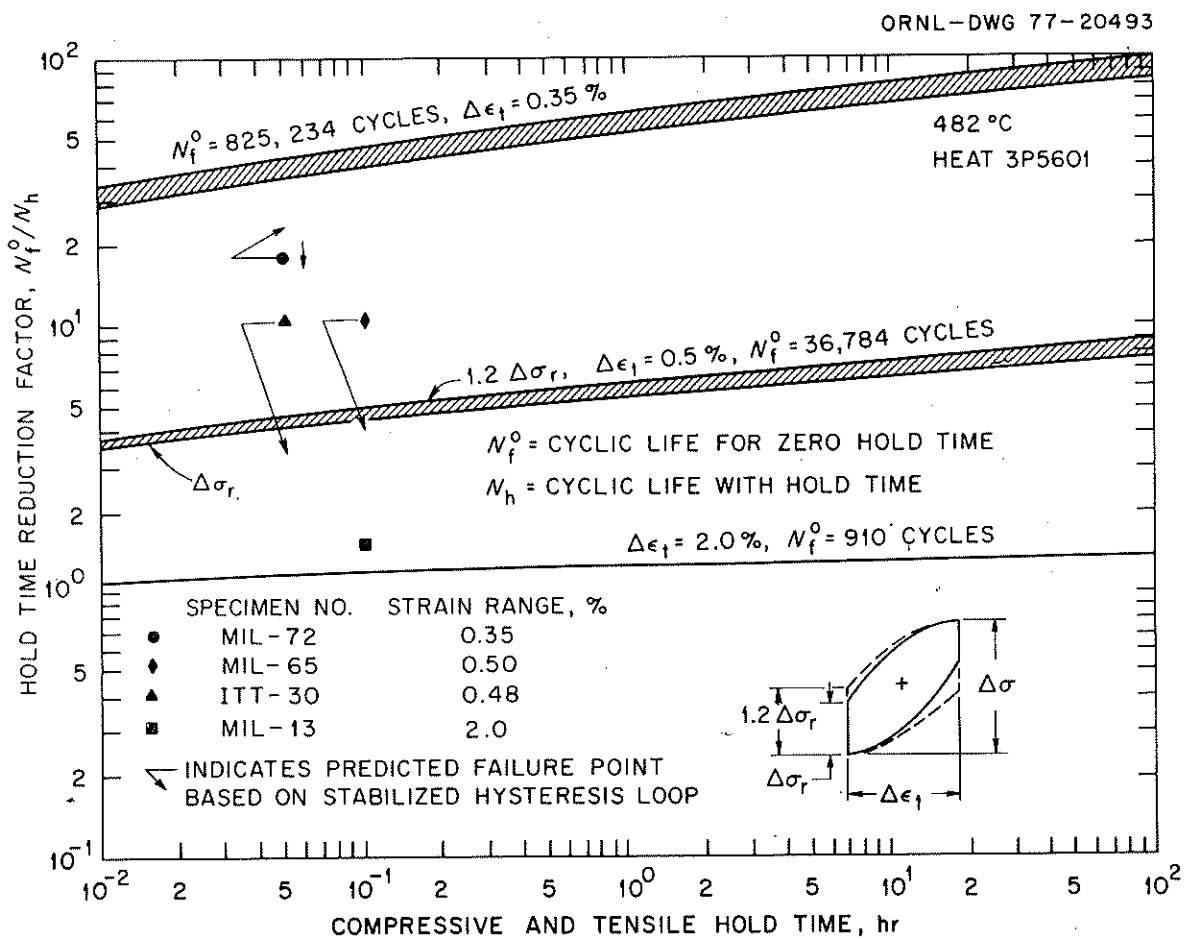


Fig. 9. Comparison of Measured and Predicted Hold-Time Reduction Factors for 2 1/4 Cr-1 Mo Steel Subjected to Both a Tensile and Compressive Hold Time of Equal Duration at 482°C.

Figures 10-13, taken as representative examples, show similar comparisons between experimentally generated strain-controlled fatigue data obtained at 538°C and predictions based on estimates of stress values from hypothetical hysteresis loops. At this temperature, however, estimates of the relaxed stress amplitude, σ , and hence the relaxed stress range, $\Delta\sigma_r$, were made by two different methods. The first method employed the Gittus equation with appropriate constants and was identical in format as previously explained for the 482°C estimates. The second method involved use of the ORNL creep equation for this material as recently developed by Booker.⁹ In the latter method of estimating relaxed stress amplitudes, the resultant predictions

are independent of the test data used for comparison purposes except for estimation of the peak stress range values, $\Delta\sigma$, which were obtained as explained previously.

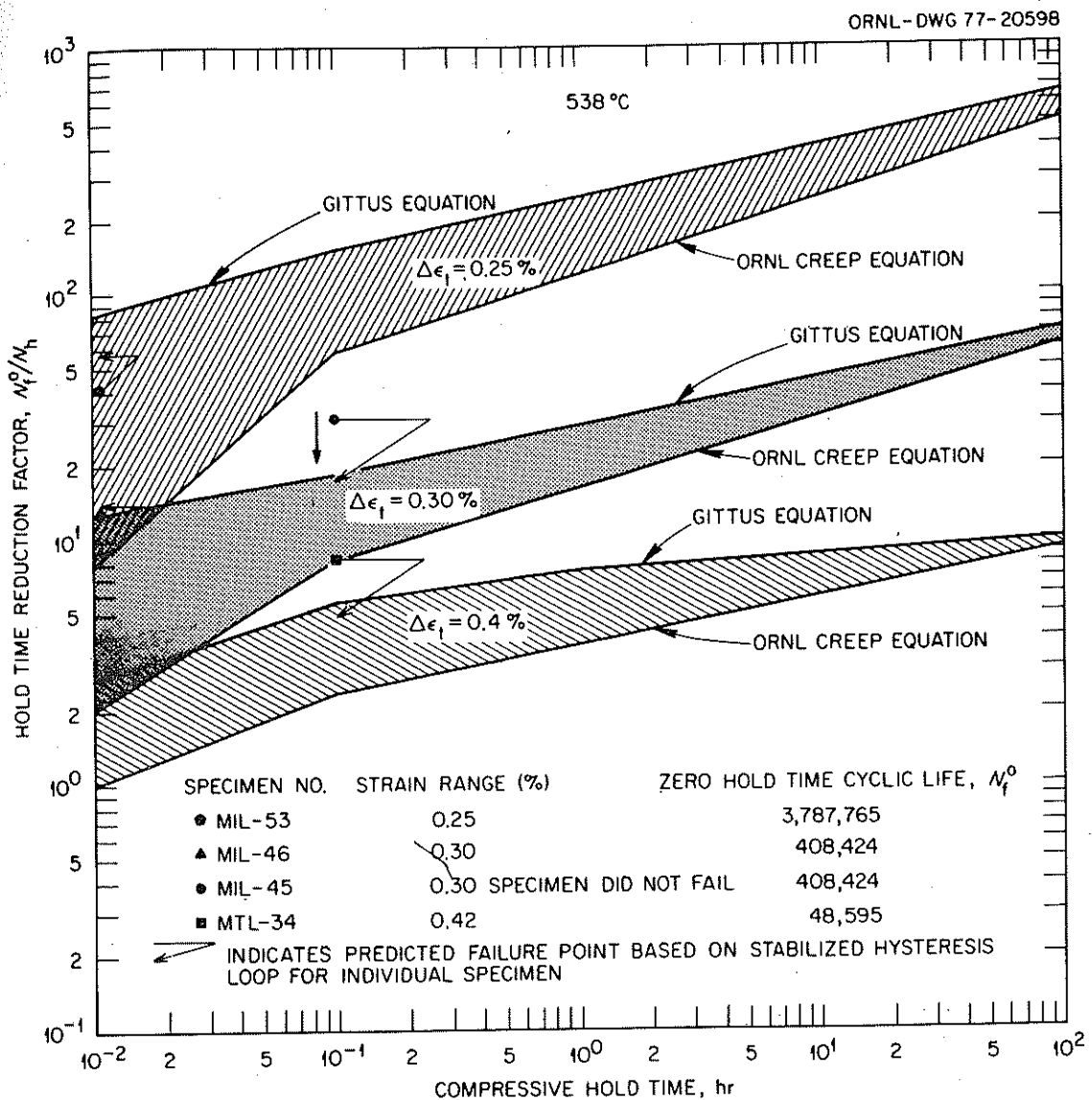


Fig. 10. Comparison of Measured and Predicted Hold-Time Reduction Factors for 2 1/4 Cr-1 Mo Steel Subjected to Compressive Hold Times at 538°C. Relaxation behavior predicted by both the ORNL creep and Gittus Equation.

ORNL-DWG 77-20793

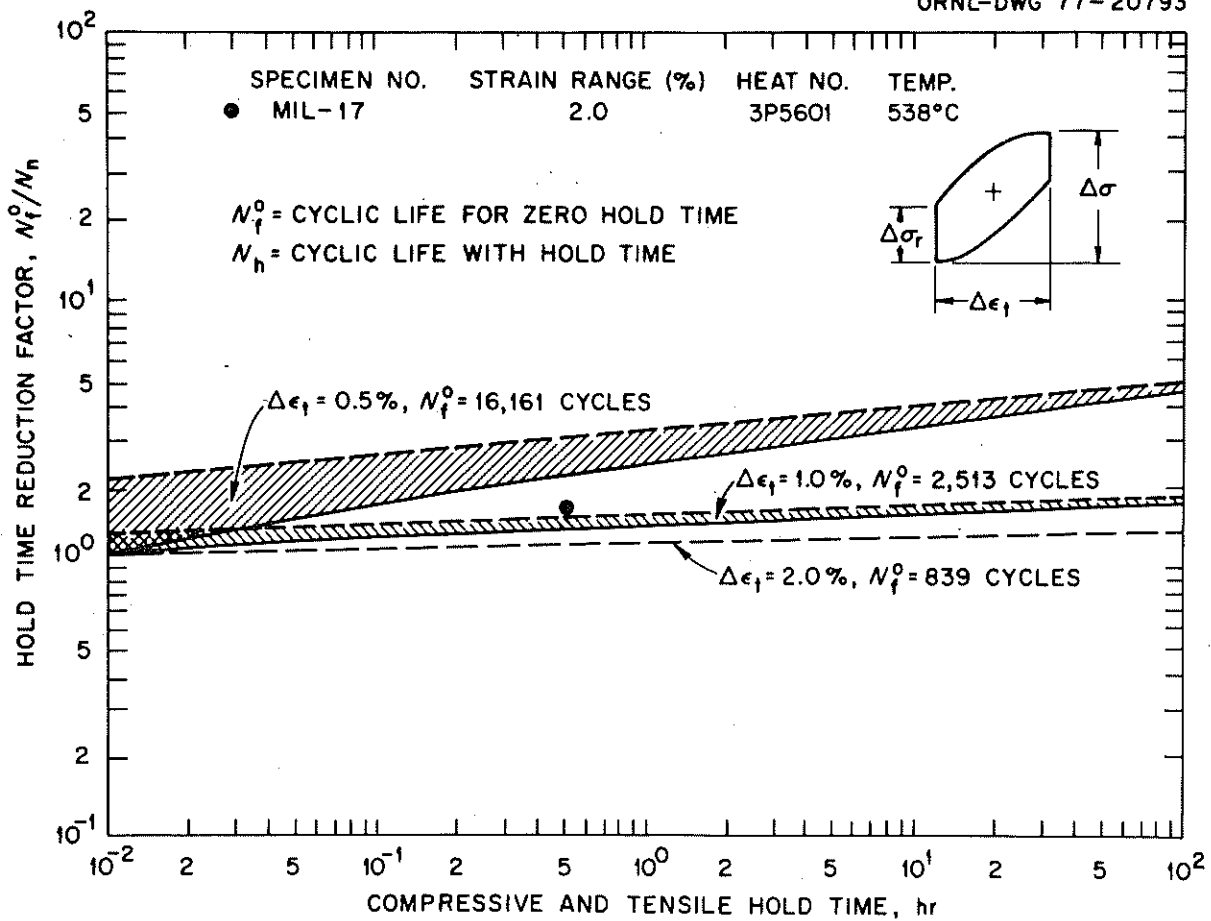


Fig. 11. Comparison of Measured and Predicted Hold-Time Reduction Factors for 2 1/4 Cr-1 Mo Steel Subjected to Both a Tensile and Compressive Hold Time of Equal Duration at 538°C.

Characteristically, the Booker creep equation tends to underpredict the amount of relaxation that occurs in the first portion of a relaxation test, while the Gittus equation may actually predict more relaxation than occurs for long hold periods. Hence, estimates obtained by these two methods in this case were used to serve as arbitrary upper and lower bounds to the resultant predictive estimates of hold-time reduction factors. Figures 10-13 show a tendency toward convergence for the two methods as the hold times approach 100 hr.

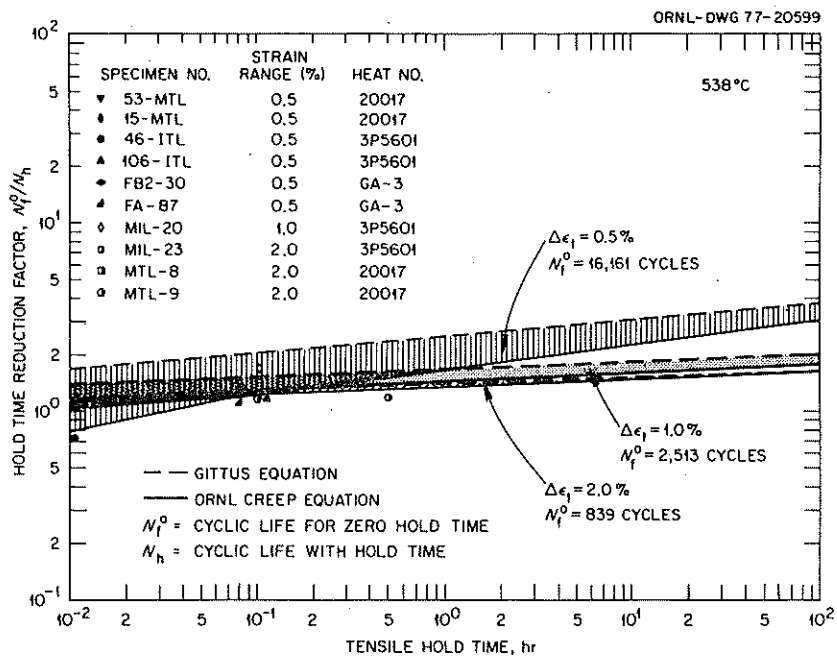


Fig. 12. Comparison of Measured and Predicted Hold Time Reduction Factors for 2 1/4 Cr-1 Mo Steel Subjected to Tensile Hold Times at 538°C. Relaxation Behavior Predicted by Both the ORNL creep and Gittus Equation.

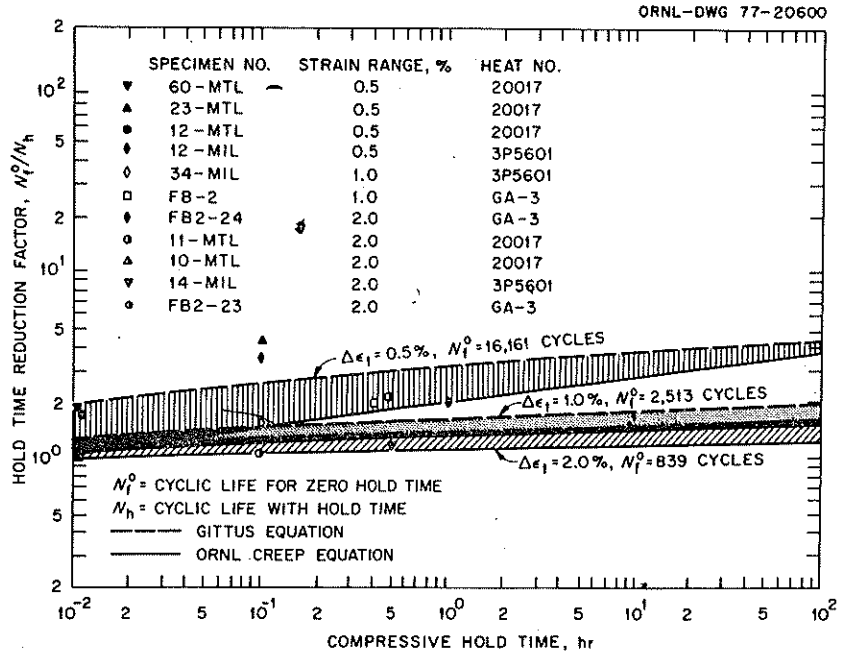


Fig. 13. Comparison of Measured and Predicted Hold Time Reduction Factors for 2 1/4 Cr-1 Mo Steel Subjected to Compressive Hold Times at 538°C. Relaxation Behavior Predicted by Both the ORNL Creep and Gittus Equation.

Hastelloy X

Results⁴ of a continuous-cycling, strain-controlled fatigue test conducted over the temperature range 649 to 871°C showed that the low-cycle (80 to about 3×10^3 cycles) fatigue life of this material was essentially independent of temperature. However, from about 3×10^3 to 10^5 cycles this same set of data indicated a temperature dependence of fatigue life, with the 871°C data falling somewhat below that of the 649°C data. These findings suggest that a single temperature-independent relationship between cycle life of N_{pp} and plastic strain range or time-independent inelastic strain range, $\Delta\epsilon_{in}$, is appropriate, particularly in the low-cycle region over this temperature interval. Indeed, when a plot of plastic strain range vs cycle life was prepared as shown in Fig. 14, this was found to be the case. Data are plotted from tests conducted at two strain

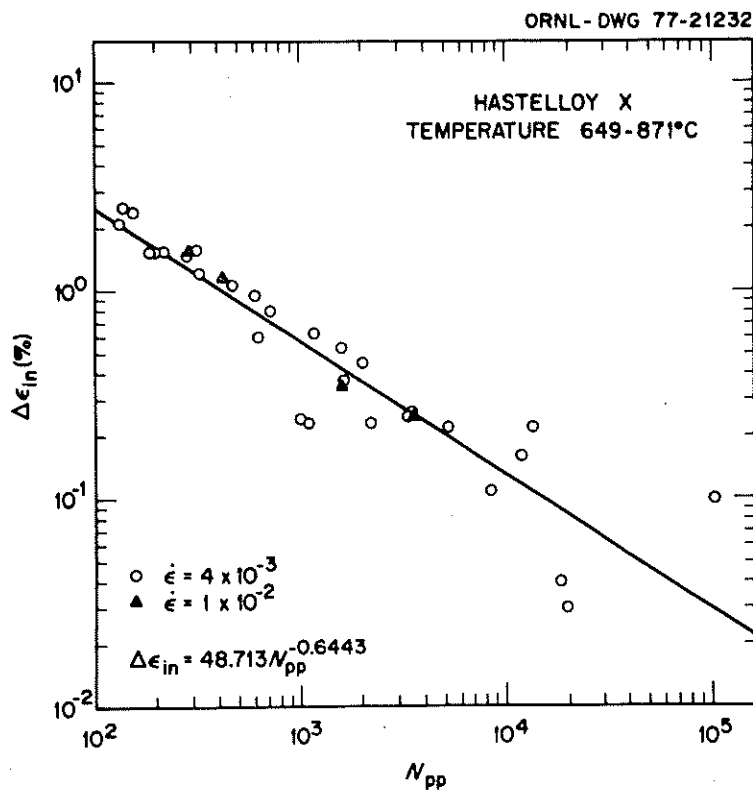


Fig. 14. Plastic Strain Range ($\Delta\epsilon_{in}$) vs Cyclic Life (N_{pp}) for a Single Heat of Hastelloy X. Indicated strain rates ($\dot{\epsilon}$) are in units of s^{-1} .

rates which indicate that cycle life is independent of strain rate for strain rates equal to or in excess of $4 \times 10^{-3}/\text{s}$. Figure 14 also shows that characteristically the scatter in the data increases with decreasing inelastic strain range.

Currently, results are available from both continuous-cycling fatigue tests as shown in Fig. 14 and from strain-controlled hold-time tests.⁴ However, the required cyclic creep tests have not been conducted to date such that the other three required life relationships could be formulated directly from applicable experimental data. Recently, however, Halford et al.¹⁰ have proposed a set of ductility normalized equations ("Universal"). These equations can be used in the absence of experimental data in conjunction with the interaction damage rule to obtain an estimate of time-dependent fatigue life of a new material for which the required life relationships were not or only partially available. Using the N_{pp} relationship given in Fig. 14 and the other three general Halford equations, the four required life relationship equations are as follows:

$$N_{pp} = 416.2 \Delta \varepsilon_{in}^{-1.55}, \quad (17)$$

$$N_{pc} = 216.1 (\Delta \varepsilon_{pc}/D_p)^{-1.67}, \quad (18)$$

$$N_{cc} = 216.1 D_c (\Delta \varepsilon_{cc})^{-1.67}, \quad (19)$$

$$N_{cp} = 148.8 D_c (\Delta \varepsilon_{cp})^{-1.67}, \quad (20)$$

where the time-independent and -dependent inelastic strain ranges, i.e., $\Delta \varepsilon_{in}$ or $\Delta \varepsilon_{pp}$, $\Delta \varepsilon_{pc}$, $\Delta \varepsilon_{cc}$, $\Delta \varepsilon_{cp}$, are in percent. D_p and D_c are true fracture tensile and creep-rupture ductilities respectively, i.e., $D = -\ln(1 - R.A./100)$, where $R.A.$ is the reduction of area given in percent.

Tensile ductility as a function of temperature is shown for Hastelloy X along with several other alloys in Fig. 15. Interim results of ongoing creep-rupture tests now in progress are given in Fig. 16 and show available creep-rupture ductilities.

Results presented in Figs. 15 and 16 show a ductility minimum in the temperature regime of about 500 to 700°C, which is also strain-rate dependent.

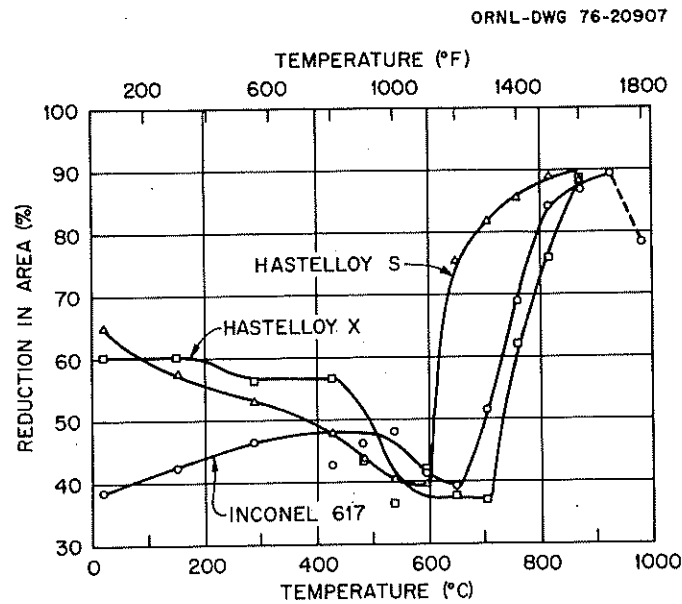


Fig. 15. Tensile Ductility of Several Superalloys. Tensile strain rates were 0.4%/min.

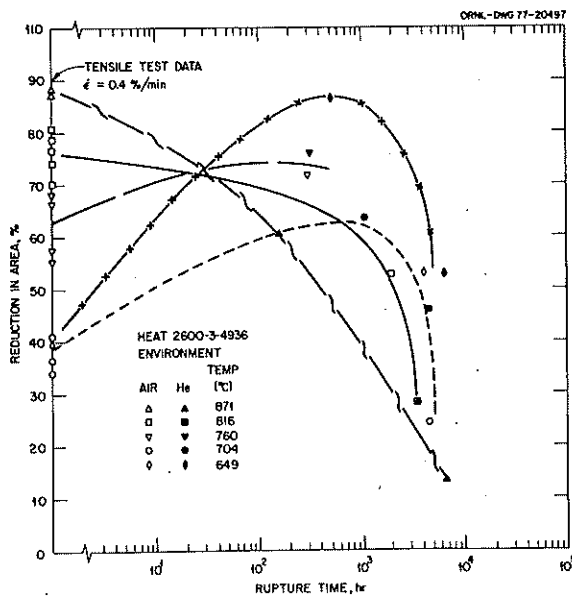


Fig. 16. Creep-Rupture Ductility as a Function of Time for Hastelloy X Tested at Several Temperatures.

Limited data from strain-controlled fully reversed fatigue tests conducted with various hold periods are available from tests conducted at 704 and 871°C.⁴ The total test time for each of these tests did not exceed several hundred hours, however, and most of the data were generated at fairly high strain ranges, i.e., 2.0, and 0.6%. Appropriate ductilities then used for estimating the cycle lives of these tests were as follows:

Temperature, °C	Tensile Ductility, R.A., %	Creep Ductility, R.A., %
704	37	50
871	68	60

Comparisons of actual vs predicted fatigue life for the available test data are given in Fig. 17. While test times as indicated above were short, the fatigue life reduction factors due to hold periods fairly small, and the data presently available limited, good agreement between actual and predicted fatigue life is apparent.

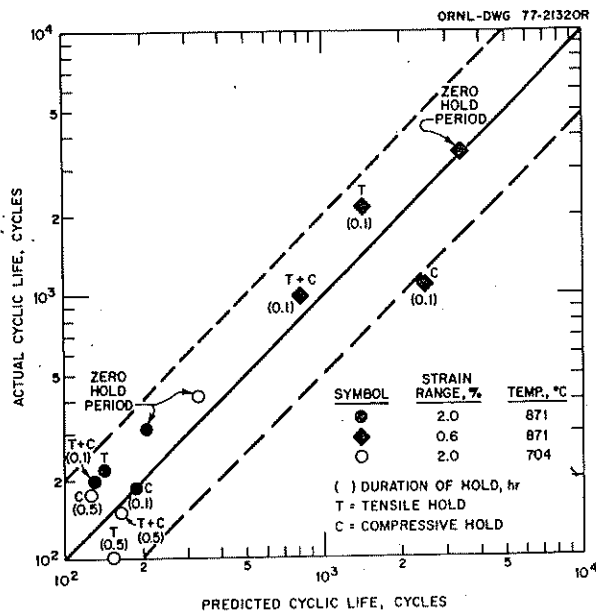


Fig. 17. Comparison of Actual and Predicted Fatigue Life for Hastelloy X Tested in Strain Control with a 0.1 to 0.5 hr Hold Period.

Type 316 Stainless Steel

Time-independent inelastic strain range, $\Delta\epsilon_{in}$, or $\Delta\epsilon_{pp}$, vs associated cyclic life, N_{pp} , values are plotted in Fig. 18 for three conditions of a single heat of type 316 stainless steel. Specific treatments given this material prior to testing

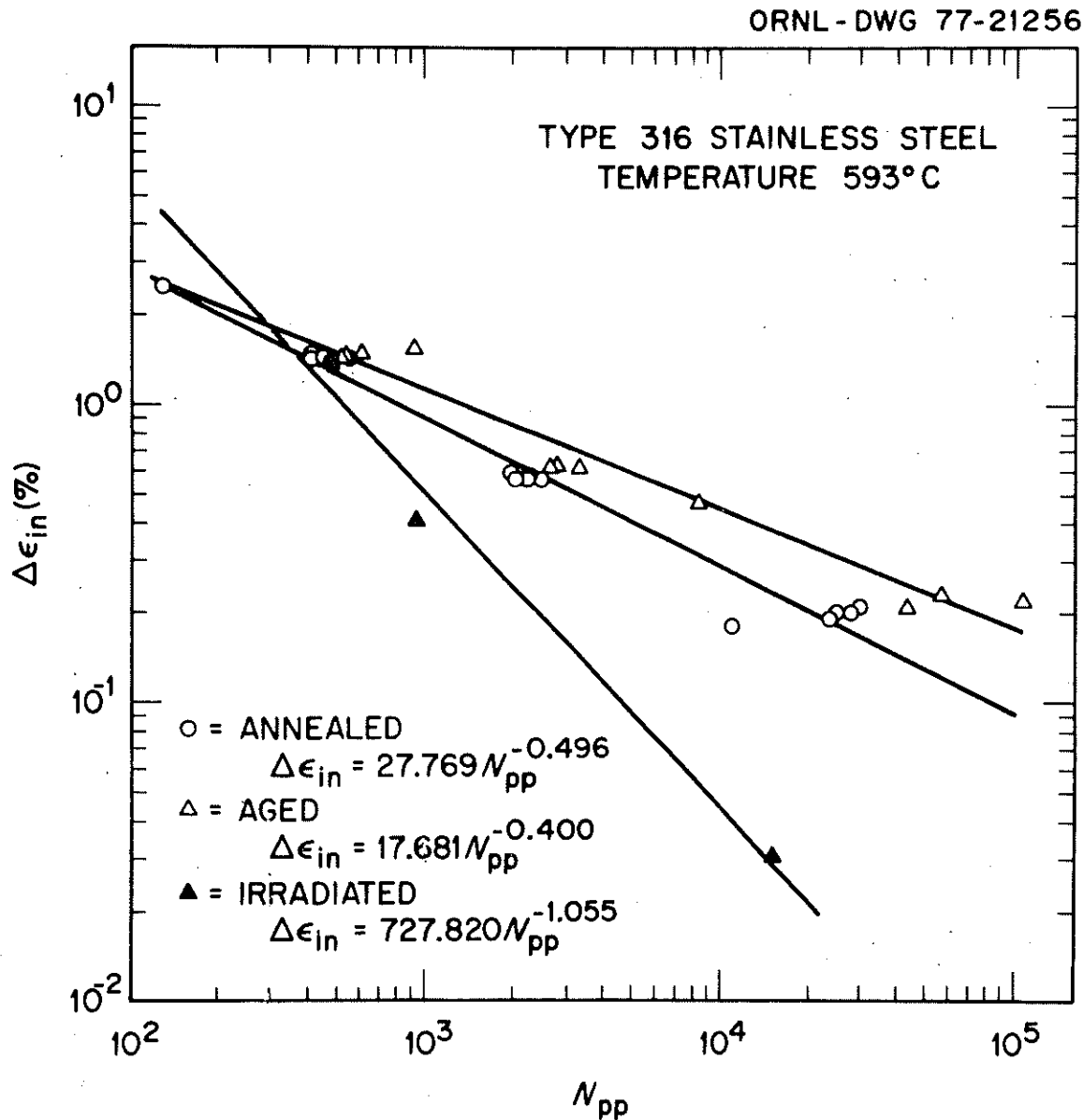


Fig. 18. Plastic Strain Range ($\Delta\epsilon_{in}$) vs Cycle Life (N_{pp}) for a Single Heat (B65808) of Type 316 Stainless Steel in Three Different Conditions.

were cited earlier in this report. All of the data^{2,3} shown in Fig. 18 were generated from continuous-cycling, strain-controlled tests conducted at 593°C at a strain rate of $4 \times 10^{-3}/\text{s}$. The effect of a preaging thermal treatment (3096 or 5040 hr at 593°C) was to displace the high-cycle portion of the solution-annealed curve upward, thereby also changing the slope of the aged relationship in comparison to the solution-annealed line. Identical tests recently conducted at 593°C on other heats of type 316 stainless steel in the solution-annealed and aged condition have also verified this aging effect.^{11,12} A comparison of the equation given in Fig. 18 for solution-annealed material was also made with test results generated on heat B65808 in the solution-annealed condition by two other laboratories.¹³ These data, however, were generated at 565°C and showed excellent agreement, indicating little temperature dependence or interlaboratory variation over this range.

Since the other three required life relationship expressions for this heat of material have not been generated to date, it was necessary to again use the ductility scaling concept. Saltsman and Halford¹⁴ have established the required relationships for another heat of type 316 stainless steel at 704°C. Accordingly, the required relationships for test waveforms involving either tensile or compressive holds expressed in terms of appropriate ductility scaling factors are as follows:

$$N_{cp} = (D_c^{593^\circ\text{C}}/D_c^{704^\circ\text{C}})^{65.88\Delta\varepsilon_{cp}^{-1.721}}, \quad (21)$$

$$N_{pc} = 395.1(\Delta\varepsilon_{pc}/D_p^{593^\circ\text{C}}/D_p^{704^\circ\text{C}})^{-1.183}, \quad (22)$$

where $\Delta\varepsilon_{cp}$ and $\Delta\varepsilon_{pc}$ are expressed in percent, and D_p and D_c are the appropriate tensile and creep ductilities respectively.

Appropriate ductilities for use in Eqs. (21) and (22) as obtained from the literature are given in Table 4. Tensile ductility of another heat (65805) of type 316 stainless steel

is included in Table 4. It shows similar behavior with respect to thermal aging in comparison to heat B65808, i.e., a decrease in tensile ductility upon aging.

Table 4. Tensile and Creep Ductilities of Several Heats of Type 316 Stainless Steel at 593 and 704°C

Heat	Temperature (°C)	Condition	Reduction of Area, %			
			Tensile	Reference	Creep	Reference
NASA	704		64	10	77	10
B65808	593	Irradiated	29	2	3	15
B65808	593	Annealed	62	3	19	15
B65808	593	Aged ^a	47	2	19 ^b	
65805	593	Annealed	72			
65805	593	Aged ^c	61			

^a5040 hr at 593°C in helium.

^bAssumed to be the same as annealed.

^c5000 hr at 593°C vacuum.

Isothermal tensile and creep ductilities for heat 65808 are plotted as a function of strain rate in Fig. 19. Ductilities for heat 8092297 are given for comparison purposes only. Tensile and creep ductilities are particularly strain-rate sensitive over the temperature range 538 to 649°C as shown by the comparisons for these two heats of type 316 stainless steel.

Using the ductilities given in Table 4, the expressions for N_{pp} given in Fig. 18, Eqs. (21) and (22), and the interaction damage rule, estimates were performed of the fatigue life of test data given in the literature.¹⁻³ Comparisons between actual and predicted cyclic lifetimes for test data available on heat B65808, involving either tensile or compressive-only hold times, are shown in Fig. 20. Particularly good agreement between actual and predicted cyclic lives, considering the many assumptions, is apparent for the data of the irradiated material.

ORNL-DWG 77-20491R

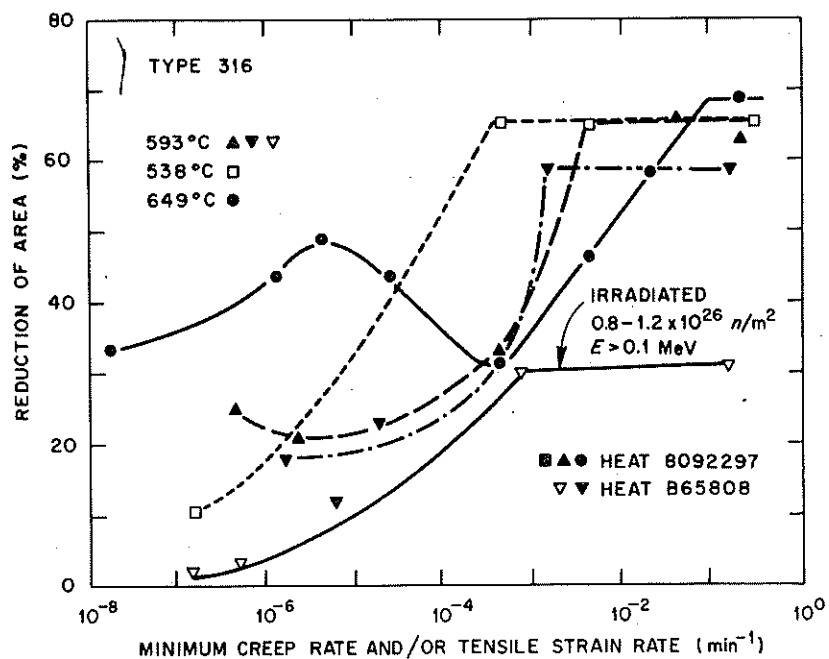


Fig. 19. Ductility of Several Heats of Type 316 Stainless Steel as a Function of Temperature and Strain Rate for Irradiated and Unirradiated Type 316 Stainless Steel.

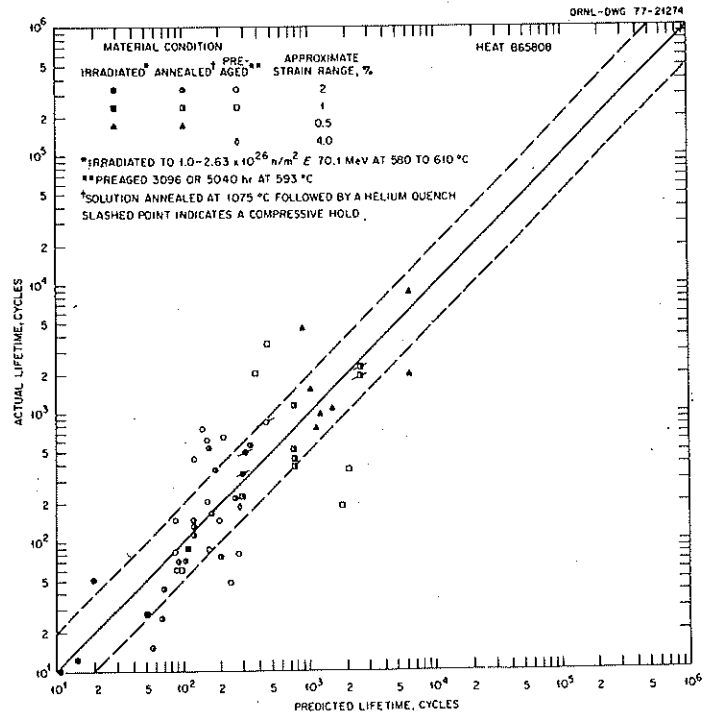


Fig. 20. Comparison of Predicted Cyclic Lifetimes Based on Strain-Range Partitioning vs Actual Cyclic Lifetimes for Type 316 Stainless Steel in Several Conditions. All tests were conducted at 565 or 593°C.

DISCUSSION

Annealed 2 1/4 Cr-1 Mo Steel

As was stated initially, the objective of this paper was to evaluate the method of strain-range partitioning as a predictive tool for estimating time-dependent fatigue behavior of several materials primarily at low strain ranges and for long hold periods. In the case of annealed 2 1/4 Cr-1 Mo steel, this was accomplished via hold-time reduction factor vs duration of strain-hold time plots (Figs. 6-13), since the method not only permits a direct comparison between predictions and available laboratory data, but also allows extrapolation to hold periods that are appropriate to the design of nuclear reactor systems. Further, plots of this type have been used historically by the formulators of ASME Code Case 1592 in establishing elastic analysis curves for time-dependent fatigue behavior.

In the authors' view, the method of strain-range partitioning was effective in predicting the general data trends, particularly for the compressive strain hold data (Figs. 6, 7, 10, and 11), apparently the most damaging mode of loading in air for this material at low strain ranges. Overall, the method was found to work very well when the various life relationships [Eqs. (3) through (7)] were accurately known.

Evaluation of strain-controlled situations at low strain ranges usually requires extrapolating the essentially load-controlled or cyclic-creep-formulated life relationships, i.e., N_{cp} , N_{pc} , and N_{cc} , down to low inelastic strain values. The available strain-controlled data suggest that little error was introduced in extrapolating the N_{pc} relationship [Eq. (5)]. However, in the case of "cc" type loading, extrapolating Eq. (4) may introduce considerable error, resulting in predicting excessive fatigue life as shown by the fact that all of the available strain-controlled data lie to the left of the "cc" life relationship line given in Fig. 2c. This suggests that either two relationships may be appropriate, i.e., one for

strain and the other for load-controlled situations, or that the data scatter is particularly large and additional data are required to modify the existing life relationship [Eq. (4)]. In the case of "pp" damage, it was shown that two equations [(6) and (7)] were required. In an effort to further substantiate this finding, continuous-cycling fatigue tests were conducted on an additional heat (50557) of 2 1/4 Cr-1 Mo steel. This heat contained a fairly low carbon content ($C = 0.026$ wt %), but the results verified the bilinear "pp" relationship as plotted on log-log coordinates. Data from this heat generally scattered throughout the existing N_{pp} life relationship data, indicating that Eqs. (6) and (7) were appropriate for the low-carbon heat as well.

Another problem area associated with the method, and for that matter any method, is that of defining the appropriate stress ranges, i.e., peak and relaxed, after long hold periods at low strain ranges. Indeed, the material may not even exhibit a stabilized hysteresis loop that is repeated from one cycle to the next after an initial period of cyclic hardening or softening. This was found to be the case for heat 20017, which exhibited cyclic softening during much of the cyclic life at low strain ranges.⁷

Defining the minimum strain range below which essentially no stress relaxation occurs after prolonged hold periods, and hence no time-dependent fatigue damage accrues, is another problem area. Figure 21 shows an experimental stress relaxation curve obtained after an initial period of cyclic hardening on heat 3P5601 at 538°C. The strain range was 0.2%. Predictions of relaxation behavior by several different methods are also given for comparison. When this same heat of material was cycled at 482°C and at a strain range of 0.30% with a compressive hold period of 0.01 hr, no relaxation occurred. Instead, the stress required to maintain a constant strain increased, as the data in Table 5 indicate.

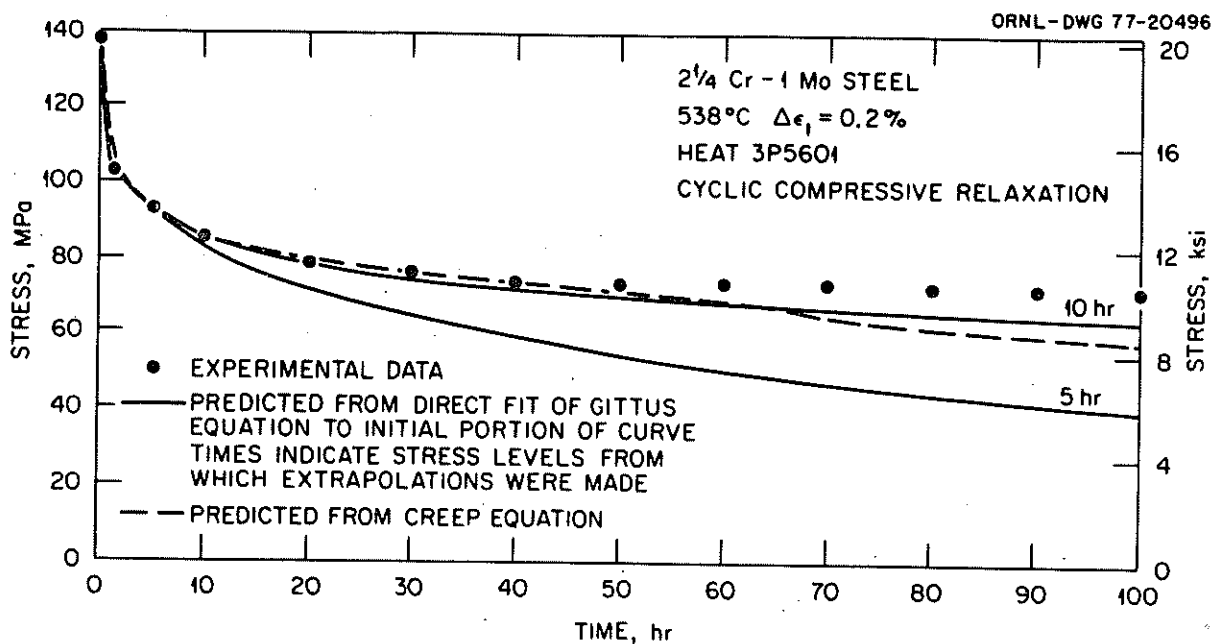


Fig. 21. Cyclic Relaxation Behavior of 2 1/4 Cr-1 Mo Steel Held at a Constant Strain Range of 0.2%. Comparisons of predicted behavior are also shown.

This phenomenon, which is ramp-rate dependent, as shown in Table 5, is thought to be due to dynamic strain aging.

Table 5. Compressive Stresses Required to Maintain a Constant Strain Range of 0.30% with a 0.01-hr Compressive Hold in Heat 3P5601 at 482°C.

Ramp Strain Rate (s^{-1})	Compressive Stress Amplitude, MPa		Inelastic Strain Range (%)	Cycle
	Beginning of Hold Period	End of Hold Period		
4×10^{-3}	193.1	204.8	0.08	405,000
4×10^{-4}	210.3	220.6	0.07	420,000
4×10^{-3}	196.5	205.5	0.08	438,000

In making estimates of long-term, time-dependent fatigue behavior of this material, no attempt was made to ductility normalize the life relationships to account for a time-dependent decrease in creep-rupture ductility. Creep-rupture ductility data available (Fig. 22) for heat 20017 suggest that this may not be necessary for temperatures in the range

of 454 to 510°C. However, heat-to-heat variations are apparent, and for temperatures much above 510°C, long-term estimates, e.g., lifetimes in excess of 10,000 hr, may require a modification factor to account for a ductility loss. Long-term cyclic and monotonic tests are under way to determine specific requirements.

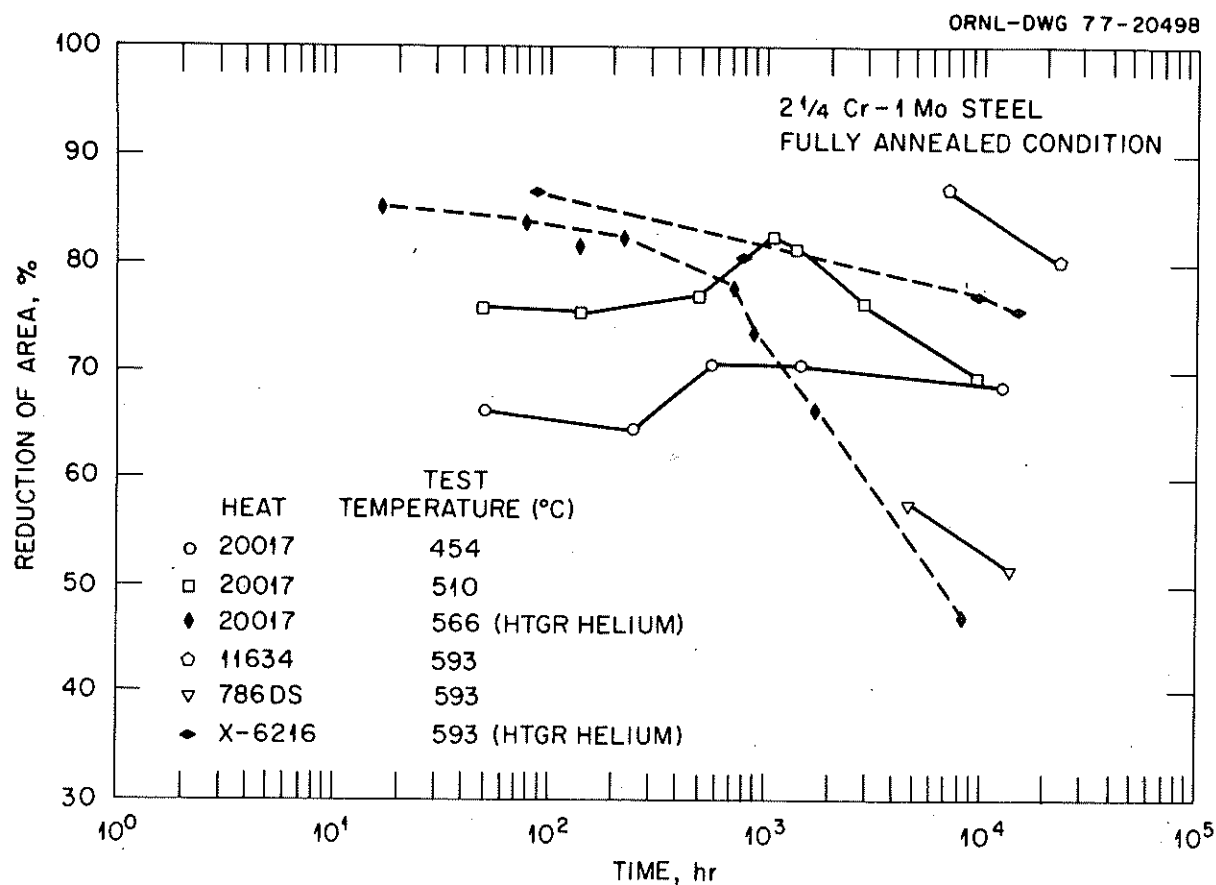


Fig. 22. Creep-Rupture Ductilities for Several Heats of 2 1/4 Cr-1 Mo Steel Tests in Air Except as Indicated.

Hastelloy X

Comparisons between expected cyclic life and actual cyclic life from tests run to date have shown excellent agreement (Fig. 17). However, test times to date have been fairly short, such that reductions in continuous-cycle fatigue life due to hold periods have not exceeded factors of about 4. Further,

additional verification tests at lower strain ranges are required, since the data have shown increased scatter at lower total and inelastic strain-range levels (Figs. 14 and 17). Further, available creep-rupture data (Fig. 16) indicate a precipitous drop in creep-rupture ductility for test times in excess of about 2000 hr. Long-term tests are required to determine whether a simple time-dependent ductility modification will indeed compensate for the low creep ductility.

Type 316 Stainless Steel

As was previously mentioned and shown in Fig. 20, rather good results were achieved in nearly every instance when comparisons were made between actual and predicted lifetimes for material in the irradiated condition. This occurred even though all of the material had not been irradiated to exactly the same fluence level. It is believed that for this material the irradiation conditions were such that the reduction in ductility and fatigue life was due primarily to the presence of agglomerated helium (bubbles) at the grain boundaries.

Comparing the relationships for $\Delta\epsilon_{in}$ vs N_{pp} for type 316 stainless steel in Fig. 18 for the three conditions, i.e., annealed, aged, and irradiated, considered herein, it is apparent that the data indicate different slopes. Scaling, then, in the case of the N_{pp} relationships by a simple ductility modification from, say, the annealed condition to the irradiated or the aged condition would have resulted in some error, since scaling displaces the relationship but does not change the slope of the life relationship line. In the case of the aged material, a prior thermal aging treatment increased the fatigue life in the intermediate

cycle regime (10^3 to 3×10^4 cycles), while the short-term tensile ductility (Table 5) actually decreased somewhat relative to the material in the annealed condition. Figure 18 indicates a crossover between the N_{pp} relationships for material in the aged or annealed condition at about 100 cycles such that the N_{pp} line for aged material lies above that of the annealed material for cyclic lives in excess of 100. Accordingly, then, a ductility modification of the annealed life relationship line to establish one for the aged material would have actually displaced the "pp" line in the wrong direction for cyclic lives in excess of about 100 cycles.

Figure 20 indicates that agreement between actual and predicted lifetimes for material in the aged and to a lesser extent in the annealed condition for tensile hold times was generally not as good as that for the corresponding comparisons for material in the irradiated condition. The reasons for this increase in scatter are not known, but of course may be due to heat-to-heat variations and the scaling assumptions necessary to obtain the required life relationship line, i.e., "cp", given as Eq. (21). Accordingly, cyclic creep tests will be initiated on this heat of material at 593°C to verify Eq. (21).

A question that one might logically ask in conjunction with the use of the ductility scaling concept is how sensitive are the predicted cycles to failure to changes in or significant errors in the estimation of appropriate ductilities. To at least partially answer this question, calculations of the predicted cyclic lives were compared for the irradiated stainless steel using the actual creep-rupture ductility, i.e., $R.A. = 3\%$ from Table 4, and a significantly higher value, i.e., $R.A. = 29\%$. Thus the creep-rupture ductility was arbitrarily assumed equal to the tensile ductility as given in Table 5. Actual cyclic life and predicted values, using the above creep-rupture ductilities, are compared in Table 6. These results from

calculations using the " N_{pp} " relationship for irradiated material given in Fig. 18, Eq. (21), and the interaction damage rule indicated that predictions were sensitive to the input ductilities.

Table 6. Comparisons between Predicted Cycles to Failure, Using Different Creep-Rupture Ductilities (R.A.) for Irradiated Type 316 Stainless Steel^a

Specimen	Total Strain Range (%)	Duration of Tensile Hold (hr)	Predicted Cycles to Failure		Actual Cycles to Failure
			R.A. = 3%	R.A. = 29%	
D-104	1.0	5.0	48	386	27
D-108	2.0	5.0	10	98	10
D-109	1.0	0.5	100	570	60
D-113	2.0	0.5	15	120	12
D-106	0.5	0.1	1125	4409	757
D-114	1.0	0.1	112	649	88

^aTest temperature was 593°C.

CONCLUSIONS

The method of strain-range partitioning was employed to predict strain-controlled, time-dependent cyclic life of a number of structural materials, including annealed 2 1/4 Cr-1 Mo steel, Hastelloy X, and irradiated and unirradiated type 316 stainless steel. The following are specific conclusions:

1. Plots of isostrain-range hold-time reduction factors vs duration of hold time were established for two heats of annealed 2 1/4 Cr-1 Mo steel at 482 and 538°C. Influence of either tension, compression, or both tension and compression strain holds was estimated for dwell periods of up to 100 hr on the continuous-cycle fatigue life. A comparison between

actual and estimated cyclic lifetimes (cycles) generally showed good agreement, particularly in the case of the compression-only strain hold situation.

2. Whereas only one of the four required life relationship equations was directly available for predicting cyclic lifetimes (cycles) for Hastelloy X, ductility scaling or normalization provided the required relationships for interim use. Comparisons between predicted and actual lifetimes (cycles) for relatively short-term experimental data generated at fairly high strain ranges at both 704 and 871°C showed good agreement.

3. Good agreement between predicted and actual cyclic lifetimes (cycles) was generally found for irradiated type 316 stainless steel. Agreement between actual and predicted cycles to failure was not so good for material in the preaged condition, i.e., up to about 5000 hr at 593°C. The increased scatter for aged material may have been due to some uncertainty in use of the available "cp" life relationship.

4. Specific problem areas or uncertainties, not necessarily unique to strain-range partitioning, that contribute to the uncertainty in making predictions for low-strain-range, long-hold-time situations were discussed and are as follows:

- a. extrapolation of life relationship equations to low inelastic strain ranges that were generated primarily from load-controlled short-term cyclic creep tests;
- b. heat-to-heat variations which cause differences in constitutive behavior;
- c. metallurgical and strain-rate-induced changes or instabilities such as thermal aging response, strain aging, and creep-rupture ductility changes;
- d. endurance limits or strain ranges below which time-dependent effects are expected to be nonexistent.

Other important factors such as cumulative damage and environmental (atmosphere) effects were not discussed in this paper but will be addressed in subsequent reports.

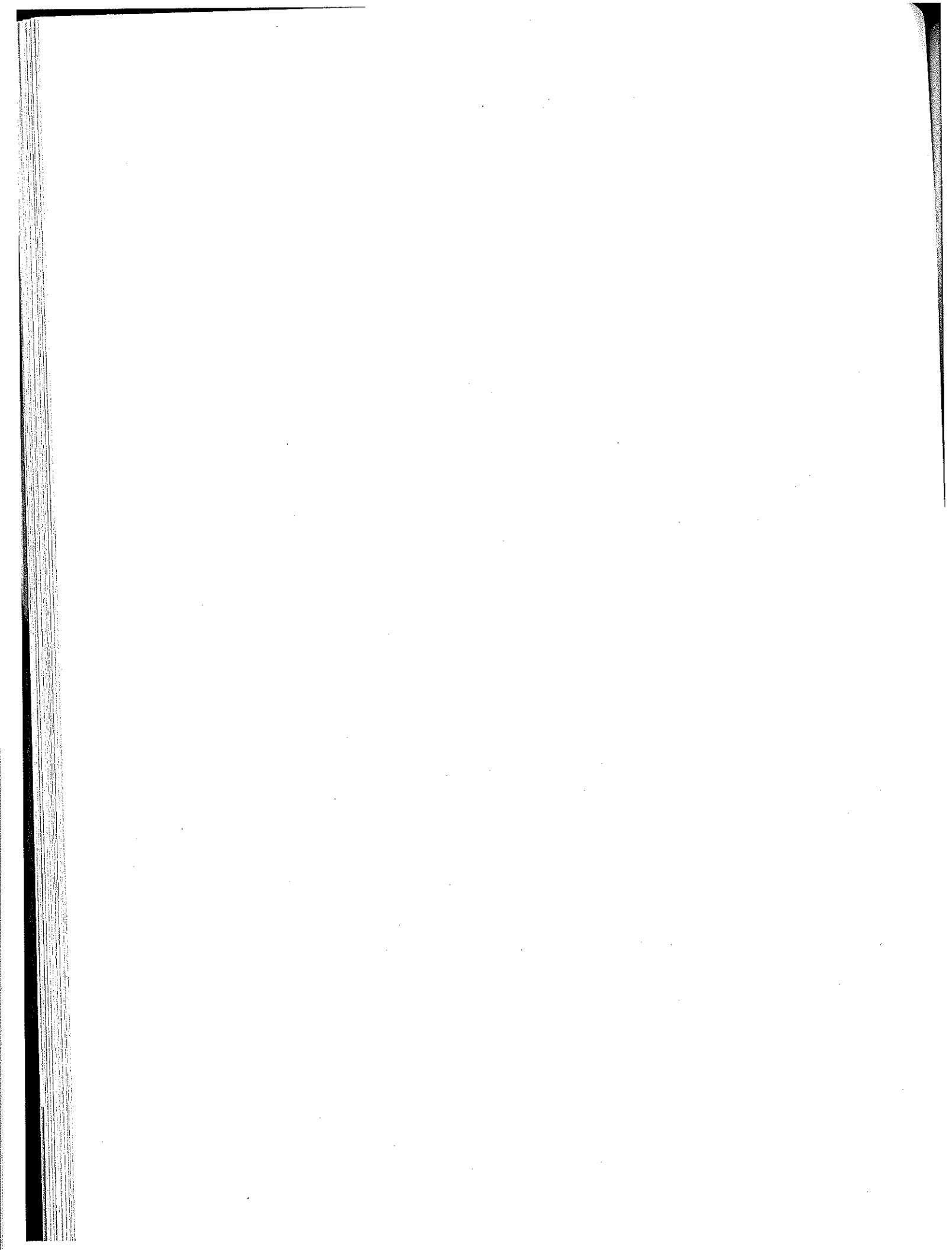
ACKNOWLEDGMENTS

The authors gratefully acknowledge the assistance of L. K. Egner in conducting the experimental tests, R. W. Swindeman and R. K. Nanstad for reviewing the paper, B. L. P. Booker for the data compilation given as Appendix A, and Fondia Burress for typing the manuscript.

REFERENCES

1. D. L. Keller, *Progress on LMFBR Cladding, Structural and Component Materials Studies During July 1971 Through June 1972, Final Report, Task 32*, BMI-1928, Battelle Columbus Laboratories.
2. C. R. Brinkman and G. E. Korth, "Low Cycle Fatigue and Hold Time Comparisons of Irradiated and Unirradiated Type 316 Stainless Steel," *Metall. Trans.* 5: 792-94 (March 1974).
3. C. R. Brinkman, G. E. Korth, and R. R. Hobbins, "Estimates of Creep-Fatigue Interaction in Irradiated and Unirradiated Austenitic Stainless Steels," *Nucl. Technol.* 16: 297-307 (October 1972).
4. C. R. Brinkman et al., *Application of Hastelloy X in Gas-Cooled Reactor Systems*, ORNL/TM-5405 (October 1976).
5. S. S. Manson, G. R. Halford, and M. H. Hirschberg, *Creep-Fatigue Analysis by Strain-Range Partitioning*, NASA TMX-67838, NASA-Lewis Research Center (1971).
6. C. R. Brinkman et al., "Time-Dependent Strain-Controlled Fatigue Behavior of Annealed 2 1/4 Cr-1 Mo Steel for Use in Nuclear Steam Generator Design," *J. Nucl. Mater.* 62(2,3): 181-204 (November 1976).
7. C. R. Brinkman et al., *Interim Report on the Continuous Cycling Elevated Temperature Fatigue and Subcritical Crack Growth Behavior of 2 1/4 Cr-1 Mo Steel*, ORNL/TM-4993, (December 1975).

8. M. H. Hirschberg and G. R. Halford, *Use of Strain-Range Partitioning to Predict High-Temperature Low-Cycle Fatigue Life*, NASA TN D-8072, NASA-Lewis Research Laboratories, January 1976.
9. M. K. Booker, *Interim Analysis of the Creep Strain-Time Characteristics of Annealed and Isothermally Annealed 2 1/4 Cr-1 Mo Steel*, ORNL/TM-5831 (June 1977).
10. G. R. Halford, J. F. Saltsman, and M. H. Hirschberg, *Ductility Normalized Strain-Range Partitioning Life Relations for Creep-Fatigue Life Predictions*, NASA/TM-73737, NASA-Lewis Research Laboratories, October 1977.
11. K. Natesan et al., "Effect of Sodium Environment on the Creep-Rupture and Low-Cycle Fatigue Behavior of Austenitic Stainless Steel," presented at the IAWA/IWGFR Specialists Meeting on Properties of Primary Circuit Structural Materials, October 17-21, 1977, Bensburg, Federal Republic of Germany.
12. P. N. Flagella, "Effects of High Temperature Sodium Exposure on the Microstructural and Time-Dependent Mechanical Behavior of Type 316 Stainless Steel," presented at the IAEA/IWGFR Specialists Meeting on Properties of Primary Circuit Structural Materials, October 17-21, 1977, Bensburg, Federal Republic of Germany.
13. D. R. Diercks, *A Compilation of Elevated-Temperature Strain-Controlled Fatigue Data on Type 316 Stainless Steel*, Argonne National Laboratory, to be published.
14. J. F. Saltsman and G. R. Halford, "Applications of Strain-Range Partitioning to the Prediction of Creep-Fatigue Lives of Types 304 and 316 Stainless Steel," presented at the ASME Joint Pressure Vessel and Piping and Petroleum Mechanical Engineering Conference, September 19-23, 1976, Mexico City, Mexico.
15. A. Ward, private communication, Westinghouse Hanford, November 1977.



Appendix A

Summary of Strain and Load
Controlled Fatigue Data
on 2 1/4 Cr-1 Mo Steel

ORNL-MARTEST CONTINUOUS CYCLING FATIGUE DATA FOR 2.25CR-1.0MOSSTEEL
STRAIN CONTROLLED

SPECIMEN NUMBER	HEAT NUMBER	TEMP DEG C	STRAIN RATE (%/SEC)	STRAIN RANGE (%)		ELASTIC STRAIN AT NF/2 (%)	PLASTIC STRAIN AT NF/2 (%)	TENSILE STRESS AMPLITUDE AT NF/2 (MPA)	COMPRESSIVE STRESS AMPLITUDE AT NF/2 (MPA)	CYCLES TO FAILURE (NFI)	CYCLES TO FAILURE (%)	TIME TO FAILURE (HRS)
				AT NF/2 (%)	AT NF/2 (%)							
294TL-A	20017	25.	0.400	3.800	0.310	0.490	334.	338.	11216.	11745.	13.	
304TL	20017	25.	0.400	3.500	0.270	0.230	292.	304.	42082.	44484.	31.	
334TL*	20017	25.	0.400	3.250	0.223	0.027	237.	248.	6702494.	841.		
294TL	20017	25.	0.400	2.000	0.400	1.600	432.	446.	1255.	1273.	4.	
354TL	20017	25.	0.400	3.290	0.246	0.344	254.	280.	63936.	612119.	247.	
324TL	20017	25.	0.400	3.350	0.250	0.100	268.	279.	150155.	154163.	75.	
404TL	20017	316.	0.400	0.700	0.300	0.400	299.	298.	14171.	15573.	17.	
554TL	20017	316.	0.400	3.500	0.290	0.210	280.	284.	29592.	35544.	25.	
414TL	20017	316.	0.400	1.200	0.350	0.850	338.	342.	3813.	4030.	7.	
544TL	20017	316.	0.400	2.000	0.395	1.605	379.	388.	1692.	1534.	4.	
424TL*	20017	316.	0.400	3.350	0.278	0.372	269.	269.	3155297.	3516755.	1300.	
674TL*	20017	316.	0.400	3.370	0.264	0.106	265.	251.	3003000.	3113553.	1209.	
564TL	20017	316.	0.400	3.420	0.285	0.135	292.	263.	218334.	2127.		
654TL	20017	316.	0.400	3.460	0.265	0.195	251.	266.	22533.	24054.	15.	
664TL	20017	316.	0.400	3.460	0.270	0.190	251.	276.	30567.	45957.	29.	
M-5	20017	371.	0.400	3.500	0.361	0.139	329.	356.	45139.	47081.	33.	
M-4	20017	371.	0.400	1.000	0.383	0.617	365.	381.	3286.	3591.	5.	
214TL	20017	427.	0.400	3.700	0.290	0.410	277.	294.	8542.	9453.	9.	
224TL	20017	427.	0.400	3.560	0.300	0.260	273.	281.	18345.	19300.	15.	
244TL	20017	427.	0.303	3.500	0.300	0.200	272.	281.	24944.	26754.	25.	
204TL	20017	427.	0.400	1.000	0.340	0.660	306.	321.	3143.	3201.	4.	
154TL*	20017	427.	0.150	1.500	0.501	0.999	431.	456.	1537.	1841.	10.	

(NEXT PAGE)

ORNL-HARTST CONTINUOUS CYCLING FATIGUE DATA FOR 2.25CR-1.0MNSTEEL
(CONTINUED)

SPECIMEN NUMBER	HEAT NUMBER	TEMP DEG C	STRAIN RATE (1/S/SEC)	ELASTIC STRAIN RANGE (%)	PLASTIC STRAIN RANGE (%)	TENSILE STRESS AMPLITUDE AT NF/2 (MPA)	COMPRESSIVE STRESS AMPLITUDE AT NF/2 (MPA)	CYCLES TO FAILURE IN NF	CYCLES TO FAILURE IN HF	TIME TO FAILURE (HRS)
				AT NF/2 (%)	AT NF/2 (%)	AT NF/2 (MPA)	IN HF (%)	IN NF (%)	IN HF (%)	IN NF (%)
18MTL	20017	427.	0.400	2.000	0.380	1.620	348.	365.	1150.	1183.
17MTL	20017	427.	0.400	2.500	0.400	2.100	362.	378.	803.	823.
374TL*	20017	427.	0.400	2.300	0.263	0.037	241.	252.	2838440.	385.
364TL	20017	427.	0.400	2.330	0.260	0.370	233.	254.	1219573.	1326239.
314TL	20017	427.	0.400	2.360	0.270	0.090	249.	253.	465164.	471052.
284TL	20017	427.	0.400	2.420	0.280	0.140	256.	267.	134531.	139410.
264TL	20017	427.	0.400	2.460	0.290	0.175	265.	276.	85807.	88669.
364TL	20017	482.	0.400	2.500	0.290	0.210	253.	270.	33043.	35152.
M-1	20017	482.	0.400	1.000	0.430	0.570	386.	394.	1958.	2154.
M-3	20017	482.	0.400	3.400	3.337	0.063	299.	308.	43069.	53885.
4MTL	20017	538.	0.400	2.700	0.310	0.390	272.	278.	5227.	5543.
5MTL	20017	538.	0.400	2.560	0.280	0.280	246.	252.	7859.	8544.
6MTL	20017	538.	0.400	2.500	0.270	0.230	236.	239.	17280.	18222.
3MTL	20017	538.	0.400	1.000	0.300	0.700	265.	267.	2464.	2558.
1MTT	20017	538.	0.400	1.000	0.310	0.690	278.	281.	2132.	2437.
2MTL	20017	538.	0.400	1.500	0.350	1.150	294.	282.	1215.	1373.
1MTL	20017	538.	0.400	2.000	0.340	1.660	295.	313.	778.	796.
2MTT	20017	538.	0.400	3.000	0.380	2.620	337.	348.	429.	444.
274TL	20017	538.	0.400	2.280	0.230	0.050	199.	206.	476059.	479174.
164TL	20017	538.	0.400	2.390	0.260	0.130	223.	237.	63238.	63620.
144TL	20017	538.	0.400	2.420	0.260	0.160	232.	232.	34353.	37626.
134TL	20017	538.	0.400	2.440	0.280	0.160	250.	252.	42503.	44540.

NEXT PAGE

ORNL-MARTEST CONTINUOUS CYCLING FATIGUE DATA FOR 2.25CP-1.0MNSTEEL
 STRAIN CONTROLLED
 (CONTINUED)

SPECIMEN NUMBER	HEAT NUMBER	TEMP DEG C	STRAIN RATE (1/S)EC)	ELASTIC STRAIN RANGE (%)	PLASTIC STRAIN RANGE AT NF/2 (%)	TENSILE STRESS AMPLITUDE AT NF/2 (MPA)	COMPRESSIVE STRESS AMPLITUDE AT NF/2 (MPA)	CYCLES TO FAILURE (NF)	CYCLES TO FAILURE (HRST)
MIL-37	20017	538.	0.400	0.460	0.270	0.190	230.	251.	26418.
MIL-39	3P5601	316.	0.400	2.000	0.350	1.650	320.	362.	1715.
MIL-38	3P5601	371.	0.400	2.000	0.360	1.640	334.	360.	1298.
MIL-5	3P5601	427.	0.400	3.700	0.280	0.420	262.	262.	8978.
MIL-11	3P5601	427.	0.400	3.600	0.270	0.330	245.	254.	9975.
MIL-7	3P5601	427.	0.400	3.550	0.260	0.290	248.	234.	22794.
MIL-50*	3P5601	427.	0.034	3.500	0.280	0.220	251.	256.	25048.
MIL-3	3P5601	427.	0.400	3.500	0.260	0.240	234.	248.	37837.
MIL-2	3P5601	427.	0.400	1.000	0.300	0.700	270.	291.	111471.
MIL-49	3P5601	427.	0.400	2.000	0.260	1.640	323.	353.	4242.
MIL-37	3P5601	427.	0.400	2.000	0.350	1.650	323.	364.	4337.
MIL-4	3P5601	427.	0.400	3.400	0.240	0.160	218.	225.	1314.
MIL-44	3P5601	482.	0.400	3.500	0.250	3.250	206.	261.	1250.
MIL-18	3P5601	482.	0.400	1.100	0.380	0.720	258.	260.	1137.
MIL-1	3P5601	482.	0.400	2.000	0.310	1.690	307.	322.	1239.
MIL-67	3P5601	482.	0.400	3.350	0.230	0.120	204.	225.	605190. TD
MIL-57	3P5601	482.	0.400	3.350	0.240	0.110	217.	229.	49373.
MIL-42	3P5601	482.	0.400	3.400	0.240	0.160	197.	240.	51656.
MIL-31U	3P5601	538.	0.400	0.500	0.220	0.280	198.	225.	883895.
MIL-10	3P5601	538.	0.400	0.500	0.220	0.280	192.	195.	766573.
MIL-48	3P5601	538.	0.400	3.250	0.200	0.050	174.	184.	13951.
MIL-21	3P5601	538.	0.400	2.000	0.300	1.700	257.	306.	2144472.
									745.
									881.
									2.

ORNL-4A TEST FATIGUE DATA FOR 2-25CR-1MO STEEL
STRAIN CONTROLLED

SPECIMEN NUMBER	TEMP DEG C	STRAIN RANGE (%)	FREQUENCY (HZ)	HOLD TIME (HRS)	PLASTIC CYCLE		TENSILE STRESS AMPLITUDE (MPA)	COMPRESSIVE STRESS AMPLITUDE (MPA)	RELAXED STRESS AMPLITUDE (MPA)	CYCLES TO FAILURE (NFI)	TIME TO FAILURE (HRS)
					STRAIN RATE (1/SEC)	STRAIN RANGE AT NF/2 (%)					
N-6	371.	0.500	0.400	0.0260	0.010	COMPRESSION	0.134	0.366	361.	339.	176.
N-7	371.	1.000	0.400	0.027	0.100	COMPRESSION	0.593	0.407	409.	351.	279.
79-MTL	427.	0.500	1.0-0.0	0.3260	0.010	TENSION	0.246	0.254	239.	255.	212.
57-4TL	427.	0.500	0.400	0.0260	0.010	COMPRESSION	0.240	0.260	266.	253.	142.
61-MTL	427.	0.500	0.400	0.3260	0.010	COMPRESSION	0.256	0.244	252.	242.	132.
3-4TT	427.	0.500	0.400	0.3260	0.010	COMPRESSION	0.220	0.260	275.	272.	225.
58-MTL	482.	0.500	0.400	0.3260	0.010	TENSION	0.265	0.215	212.	224.	190.
64-MTL	482.	0.500	0.400	0.3260	0.010	TENSION	0.278	0.222	215.	234.	172.
77-MTL	482.	0.500	0.400	0.355	0.050	COMPRESSION	0.300	0.280	212.	150.	348.
80-MTL	482.	0.500	0.400	0.3260	0.010	COMPRESSION	0.260	0.240	237.	225.	120.
72-4TL	482.	0.500	0.400	0.3260	0.010	COMPRESSION	0.270	0.230	225.	194.	11026.
76-MTL	482.	0.500	0.400	0.3260	0.010	TENSION	0.270	0.230	225.	189.	86.
35-MTL	482.	0.500	0.400	0.3260	0.010	COMPRESSION	0.250	0.241	238.	241.	7205.
4-4TT	482.	0.500	0.400	0.3260	0.010	COMPRESSION	0.270	0.230	231.	227.	138.
44-4TL	482.	0.500	0.400	0.3260	0.010	COMPRESSION	0.274	0.226	238.	226.	11110.
H-6	482.	0.500	0.400	0.3055	0.050	COMPRESSION	0.220	0.280	219.	234.	16.
H-9	482.	0.500	0.400	0.3028	0.100	COMPRESSION	0.260	0.240	249.	232.	773.
N-2	482.	1.000	0.400	0.0027	0.100	COMPRESSION	0.702	0.298	305.	226.	1347.
N-15	482.	0.400	0.400	0.3260	0.010	COMPRESSION	0.180	0.220	222.	182.	239.
60-MTL	538.	0.500	0.400	0.0260	0.010	COMPRESSION	0.317	0.183	197.	140.	8662.
53-MTL	538.	0.500	0.400	0.3260	0.010	TENSION	0.300	0.200	204.	195.	92.
											16003.
											171.
											157.

(NEXT PAGE)

DRNL-MARTEST FATIGUE DATA FOR 2.25CR-1MO STEEL
(CONTINUED)

SPECIMEN NUMBER	TEMP DEG C	STRAIN RANGE (%)	FREQUENCY (HZ)	HOLD TIME (HRS)	PLASTIC STRAIN		TENSILE STRESS AMPLITUDE (MPA)		COMPRESSIVE STRESS AMPLITUDE (MPA)		CYCLES TO FAILURE (NFI)	TIME TO FAILURE (HRS)
					RATE (%/SEC)	RANGE AT NF/2 (%)	AT NF/2 (MPA)	AMPLITUDE (MPA)	RELAXED STRESS (MPA)			
12-MTL	538.	0.500	0.400	0.0260	0.010	COMPRESSION	0.280	0.220	221.	172.	9284.	98.
23-MTL	538.	0.500	0.400	0.0268	0.100	COMPRESSION	0.300	0.203	223.	205.	139.	3846.
15-MTL	538.	0.500	0.400	0.0260	0.010	TENSION	0.290	0.210	224.	239.	142.	13091.
11-MTL	538.	2.000	0.400	0.0267	0.100	COMPRESSION	1.740	0.250	290.	290.	167.	765.
10-MTL	538.	2.000	0.400	0.0217	0.010	COMPRESSION	1.710	0.253	294.	304.	230.	828.
9-MTL	538.	2.000	0.400	0.0267	0.100	TENSION	1.730	0.270	250.	309.	162.	717.
8-MTL	538.	2.000	0.400	0.0217	0.010	TENSION	1.710	0.290	292.	313.	220.	753.
34-MTL	538.	0.420	0.500	0.0268	0.100	COMPRESSION	0.230	0.193	204.	195.	144.	5983.
MIL-6	427.	0.500	0.400	0.0260	0.010	COMPRESSION	0.265	0.235	229.	225.	205.	29407.
MIL-29	427.	1.000	0.400	0.0267	0.100	COMPRESSION	0.730	0.273	270.	283.	225.	2355.
MIL-26	482.	0.500	0.400	0.0260	0.010	COMPRESSION	0.280	0.220	224.	221.	187.	10178.
MIL-27	482.	0.500	0.400	0.0268	0.100	COMPRESSION	0.290	0.210	211.	213.	175.	6111.
MIL-36	482.	0.500	0.400	0.0268	0.100	TENSION	0.290	0.213	232.	215.	158.	20147.
MIL-43	482.	0.500	0.400	0.0211	0.010	COMPRESSION	0.300	0.203	209.	209.	159.	5448.
MIL-24	482.	1.000	0.400	0.0267	0.100	COMPRESSION	0.750	0.250	257.	262.	156.	1924.
MIL-30	482.	1.000	0.400	0.0206	0.500	TENSION	0.790	0.210	207.	252.	133.	1633.
MIL-35	482.	1.000	0.400	0.0027	0.100	TENSION	0.770	0.230	247.	255.	162.	2058.
MIL-22	482.	1.025	0.400	0.0006	0.500	COMPRESSION	0.795	0.230	252.	253.	172.	1626.
MIL-16	482.	2.000	0.400	0.0006	0.500	COMPRESSION	1.725	0.275	314.	309.	192.	768.
MIL-13	482.	2.000	0.400	0.0014	0.100	SHEATH	1.775	0.225	287.	305.	197.	571.
MIL-23	482.	2.000	0.413	0.0006	0.500	TENSION	1.720	0.280	315.	315.	170.	357.

(NEXT PAGE)

ORNL-MAPTEST FATIGUE DATA FOR 2.25CR-1Mn STEEL
(CONTINUED)

SPECIMEN NUMBER	TEMP DFG C	STRAIN RANGE (%)	FREQUENCY (HZ)	HOLD TIME (HRS)	HOLD MODE		PLASTIC STRAIN RANGE AT MF/2	TENSILE STRESS AMPLITUDE (MPA) AT MF/2	COMPRESSIVE STRESS AMPLITUDE (MPA) AT MF/2	RELAXED STRESS AMPLITUDE (MPA)	CYCLES TO FAILURE (NF)	TIME TO FAILURE (HPS)	
					COMPRESSION	TENSION							
MIL-25	482.	2.000	0.400	0.0006	0.500	0.100	1.720	0.280	306.	310.	202.	827.	
MIL-9	482.	2.000	0.400	0.3027	0.100	1.710	0.200	301.	321.	212.	741.	76.	
MIL-8	482.	2.000	0.400	0.2027	0.100	1.723	0.280	303.	304.	208.	889.	91.	
MIL-54	482.	0.250	0.400	0.3055	0.050	1.724	0.140	0.210	206.	188.	179.	34995.	1767.
MIL-70	482.	0.350	0.400	0.3265	0.010	1.730	0.220	206.	203.	157.	83343.	874.	
MIL-21	482.	0.420	0.400	0.3450	0.030	1.730	0.210	0.190	187.	185.	155.	15539.	505.
MIL-40	482.	0.400	0.400	0.3055	0.050	1.730	0.190	0.210	208.	210.	174.	15326.	775.
MIL-41	482.	0.430	0.400	0.3263	0.010	1.730	0.180	0.220	205.	219.	183.	26176.	276.
MIL-28U	538.	0.500	0.400	0.3760	0.010	1.730	0.352	0.148	185.	155.	111.	5300.	57.
MIL-12	538.	0.500	0.400	0.3260	0.100	1.730	0.330	0.170	191.	177.	122.	4496.	453.
MIL-52	538.	0.250	0.430	0.3268	0.010	1.730	0.080	0.170	156.	157.	150.	92980.	962.
MIL-34	538.	1.000	0.400	0.3027	0.100	1.730	0.810	0.190	215.	211.	124.	1577.	160.
MIL-20	538.	1.000	0.400	0.3027	0.100	1.730	0.810	0.190	221.	212.	121.	1499.	152.
MIL-17	538.	2.000	0.400	0.3003	0.500	1.730	1.870	0.130	243.	255.	115.	533.	535.
MIL-15	538.	2.000	0.400	0.3006	0.500	1.730	1.790	0.210	238.	265.	108.	640.	322.
MIL-14	538.	2.000	0.400	0.3006	0.500	1.730	1.770	0.230	271.	267.	129.	714.	255.
MIL-46	538.	0.300	0.400	0.3267	0.010	1.730	0.130	0.170	168.	155.	133.	32284.	336.
MIL-45	538.	0.300	0.400	0.3028	0.100	1.730	0.135	0.165	172.	153.	124.	13131.	1319.

ORNL-BMI FATIGUE DATA FOR 2.25CR-1.0MO STEEL
LOAD CONTROLLED

SPECIMEN NUMBER	HEAT NUMBER	TEMP DEG C	FREQUENCY (HZ)	STRESS RANGE (MPA)	MEASURED STRAIN RANGE AT NF/2		CYCLES TO FAILURE (NF)
					FROM CYCLIC STRESS-STRAIN CURVE (%)	AT NF/2 FROM YOUNG'S MODULUS	
M-13*	20017	316.	2.0000	64000.0	0.2700	0.2500	0.2340 141370.
M-11*	20017	316.	20.0000	66000.0	0.2600	0.2700	0.2410 215000.
69MTL*	20017	316.	20.0000	66000.0	0.2100	0.2700	0.2410
74MTL	20017	316.	20.0000	68000.0	0.2800	0.2800	0.2480 130900.
M-14*	20017	316.	2.0000	68400.0	0.4700	0.2800	0.2500 46170.
M-10*	20017	316.	20.0000	70000.0	0.3600	0.3000	0.2550 25200.
73MTL	20017	316.	20.0000	72000.0	0.3200	0.3200	0.2530 43200.
50MTL	20017	316.	20.0000	80000.0	0.5000	0.2920	0.2920 4700.
48 MTL	20017	427.	20.0000	60000.0	0.2500	0.2330	45328192.
49 MTL	20017	427.	20.0000	64000.0	0.2800	0.2490	20229200.
46 MTL	20017	427.	20.0000	66000.0	0.2900	0.2570	7102780.
47 MTL	20017	427.	20.0000	68000.0	0.3000	0.2640	2983600.
71MTL*	20017	427.	2.0000	70000.0	0.2900	0.3200	0.2720
72MTL	20017	427.	20.0000	70000.0	0.2700	0.3200	0.2720 15487600.
43MTL	20017	427.	0.3330	74000.0	0.3682		187836.
70MTL*	20017	427.	2.0000	74000.0	0.2900	0.3700	0.2880
45MTL	20017	427.	20.0000	74000.0	0.2900	0.3500	16300.
52MTL	20017	427.	50.0000	74000.0	0.3500		10000.

ORNL-8MI FATIGUE DATA FOR 2.25CR-1.0MO
STEEL
LOAD CONTROLLED

SPECIMEN NUMBER	COMMENTS
M-13*	TEST RIV IN STRAIN CONTROL(1.% STRAIN RANGE)FOR FIRST 20 CYCLES.
M-11*	FQ INCREASED FROM 1 AFTER 1000 CYCLES; MEAN STRAIN 0.1-0.4; ED=ABOUT 64000 FO R FIRST 300 CYCLES
69MTL*	AXIAL STRAIN RANGE=0.21% WHEN TEST STOPPED AT 7727500 CYCLES; FQ INCREASED FROM 1 AFTER 1000 CYCLES
74MTL	FQ INCREASED FROM 1 AFTER 1000 CYCLES; MEAN STRAIN ABOUT +0.07%
M-14*	TEST RIV IN STRAIN CONTROL(STRAIN=.16% TO CYCLE 245, THEN .33% TO CYCLE 470, THEN .35% TO CYCLE 750)
M-10*	FQ INCREASED FROM 1 AFTER 1000 CYCLES; MEAN STRAIN ABOUT +0.15%
73MTL	
50MTL	
48 MTL	STRAIN RANGE FROM DYNAMIC MODULUS=0.2238
49 MTL	STRAIN RANGE USING DYNAMIC MODULUS=0.239
46 MTL	STRAIN RANGE FROM DYNAMIC MODULUS=0.246
47 MTL	STRAIN RANGE FROM DYNAMIC MODULUS=0.2537
71MTL*	NO FAIL, TEST SUSPENDED
72MTL	
43MTL	
70MTL*	NO FAIL, TEST SUSPENDED
45MTL	
52MTL	

ORNL-BMI CONTINUOUS CYCLING FATIGUE DATA FOR 2.25CR-1-MO STEEL
STRAIN CONTROLLED

SPECIMEN NUMBER	HEAT NUMBER	TEMP DEG C	STRAIN RATE (%/SEC)	STRAIN RANGE (%)	ELASTIC STRAIN RANGE AT NF/2 (%)	PLASTIC STRAIN RANGE AT NF/2 (%)	CYCLES TO FAILURE (NF)	TIME TO FAILURE (HR)
BIL-3	3P5601	316.	0.040	0.490	0.260	0.230	25737.	175.
BIL-6*	3P5601	317.	0.004	0.490	0.270	0.220	26915.	1832.
BIL-2	3P5601	317.	0.400	0.500	0.260	0.240	32514.	23.
BIL-2	3P5601	427.	0.040	0.510	0.260	0.250	37996.	269.
BIL-1	3P5601	427.	0.400	0.500	0.280	0.220	38770.	27.
BIL-13	3P5601	482.	0.400	0.500	0.220	0.280	24035.	1218.
BIL-14	3P5601	538.	0.004	0.770	0.210	0.560	1463.	156.
BIL-9	3P5601	538.	0.004	0.500	0.200	0.300	5169.	359.
BIL-4	3P5601	538.	0.004	1.020	0.230	0.790	1500.	213.
BIL-19	3P5601	538.	0.004	1.990	0.280	1.710	360.	97.
BIL-11	3P5601	538.	0.400	0.500	0.270	0.230	16185.	11.
BIL-15	3P5601	538.	0.400	1.030	0.270	0.760	2477.	4.
BIL-16	3P5601	538.	0.400	2.090	0.360	1.730	846.	2.

FRNL CONTINUOUS CYCLING FATIGUE DATA FOR 2.25CR-1.5M STEEL
STRAIN CONTROLLED

SPECIMEN NUMBER	HEAT NUMBER	TFMP DFG C	STRAIN RATE (1/SEC)	STRAIN RANGE (%)	PLASTIC STRAIN AT NF/2 (%)	TENSILE STRESS AMPLITUDE AT NF/2 (MPA)	TIME TO FAILURE INF	
							CYCLES TO FAILURE INF	TIME TO FAILURE (HPSI)
R73	20017	24.	0.400	0.500	0.240	.0.260	297.	22.
R65	20017	24.	0.400	1.000	0.384	0.616	284.	349.
21RFL	20017	25.	0.400	0.800	0.334	0.466	327.	338.
24BFL	20017	25.	0.400	0.500	0.295	0.205	296.	295.
4A2	20017	25.	0.400	2.000	0.445	1.555	420.	423.
2A2	20017	25.	0.400	2.000	0.468	1.532	398.	403.
26BFL	20017	25.	0.400	2.000	0.400	1.600	425.	425.
R6003	20017	93.	0.400	2.003	0.421	1.582	386.	366.
R6008	20017	316.	0.400	0.500	0.322	0.178	248.	257.
46RFL	20017	371.	0.004	1.000	0.379	0.621	346.	358.
36BFL	20017	371.	0.004	2.000	0.433	1.567	343.	368.
3BFT	20017	371.	0.400	0.800	0.387	0.413	315.	315.
R6001	20017	371.	0.400	0.501	0.331	0.169	260.	265.
22BFL*	20017	371.	0.400	0.500	0.314	0.186	264.	274.
I19	20017	371.	0.400	0.500	0.273	0.227	267.	272.
R54	20017	371.	0.400	0.500	0.239	0.261	124.	133.
47BFL	20017	371.	0.400	1.000	0.390	0.610	346.	341.
44BFL	20017	371.	0.400	2.000	0.430	1.570	412.	406.
I16	20017	371.	0.400	2.000	0.402	1.598	350.	367.
R63	20017	371.	0.400	0.400	0.309	0.091	223.	234.
I6018	20017	538.	0.400	0.720	0.290	0.430	222.	276.
I6016	20017	538.	0.400	0.710	0.280	0.430	250.	226.
I6077	20017	538.	0.400	0.560	0.250	0.310	231.	209.

(NEXT PAGE)

CONTINUOUS CYCLING FATIGUE DATA FOR 2.25Cr-1.5Mo STEEL
 STRAIN CONTROLLED

(CONTINUED)

SPECIMEN NUMBER	HEAT NUMBER	TEMP DEG C	STRAIN RATE (2/SEC)	STRAIN RANGE (%)	ELASTIC STRAIN (%)	PLASTIC STRAIN (%)	TENSILE STRESS AMPLITUDE AT NF/2 (MPA)	CYCLES TO FAILURE (NF)	TIME TO FAILURE (HRS)
IIL-22	20017	538.	0.400	0.500	0.229	0.271	213.	219.	22353.
R6007	20017	538.	0.400	1.000	0.250	0.750	224.	1508.	79.
I6006	20017	538.	0.400	1.000	0.270	0.720	243.	1252.	29.
I603T	20017	538.	0.400	1.020	0.310	0.710	241.	286.	1264.
I609T	20017	538.	0.400	2.000	0.230	1.770	209.	210.	534.
I608T	20017	538.	0.400	2.000	0.320	1.680	246.	309.	313.
I604T	20017	538.	0.400	2.000	0.310	1.690	241.	300.	440.
I6009	20017	538.	0.400	2.000	0.310	1.690	305.	243.	504.
I602T	20017	538.	0.400	2.970	0.350	2.620	250.	364.	158.
I606T	20017	538.	0.400	2.970	0.320	2.650	312.	248.	320.
IUL-16	3P5601	25.	0.400	0.510	0.256	0.256	254.	275.	32403.
IUL-18	3P5601	25.	0.400	1.004	0.300	0.700	310.	310.	4079.
IIL-76	3P5601	25.	0.400	1.017	0.318	0.698	324.	332.	4042.
IUL-14	3P5601	25.	0.400	1.980	0.357	1.626	367.	370.	1047.
ITT-5	3P5601	25.	0.400	2.000	0.368	1.733	369.	390.	958.
ITT-75	3P5601	25.	0.400	2.007	0.382	1.656	385.	402.	724.
ITT-77	3P5601	25.	0.400	2.120	0.374	1.750	376.	397.	712.
ITT-6	3P5601	25.	0.400	0.350	0.230	0.120	234.	252.	140235.
IUL-15	3P5601	25.	0.400	0.350	0.237	0.113	246.	244.	115122.
I10	3P5601	371.	0.400	0.600	0.293	0.307	261.	272.	18568.
IIL-38	3P5601	371.	0.400	0.503	0.289	0.214	252.	232.	30566.
IIL-32	3P5601	371.	0.400	0.502	0.281	0.221	242.	258.	29363.
14	3P5601	371.	0.400	1.000	0.332	0.668	295.	305.	4303.

{NEXT PAGE}

ORNL CONTINUOUS CYCLING FATIGUE DATA FOR 2.25CR-1.5MN STEEL
(CONTINUED)

SPECIMEN NUMBER	HEAT NUMBER	TEMP DEG C	STRAIN RATE (1/SFC)	STRAIN RANGE (%)	ELASTIC STRAIN (%)	PLASTIC STRAIN (%)	TENSILE STRESS AMPLITUDE AT NF/2 (MPA)	COMPRESSIVE STRESS AMPLITUDE AT NF/2 (MPA)	CYCLES TO FAILURE (NF)	TIME TO FAILURE (HRS)
117	3P5601	371.	0.400	1.000	0.324	0.676	305.	325.	3310.	46.
120	3P5601	371.	0.400	1.250	0.336	0.914	319.	330.	2711.	6.
111	3P5601	371.	0.400	1.500	0.409	1.091	326.	348.	2028.	4.
17	3P5601	371.	0.400	1.750	0.355	1.305	339.	352.	1470.	4.
13	3P5601	371.	0.400	0.350	0.250	0.100	235.	257.	417225.	203.
12	3P5601	371.	0.400	0.400	0.200	0.101	241.	257.	157252.	87.
AP08	3P5601	427.	0.400	0.520	0.244	0.276	222.	228.	22700.	16.
AP02U	3P5601	427.	0.400	0.250	0.190	0.060	171.	178.	1339362.	465.
AP13	3P5601	427.	0.400	1.000	0.291	0.709	265.	271.	3112.	4.
AP14	3P5601	427.	0.400	2.000	0.346	1.654	315.	322.	874.	2.
AP01	3P5601	427.	0.400	0.300	0.212	0.088	194.	197.	1858212.	770.
AP10	3P5601	427.	0.400	0.400	0.232	0.168	213.	214.	112028.	62.
ITL-15	3P5601	482.	0.004	0.500	0.196	0.304	198.	212.	7234.	502.
ITL-16	3P5601	482.	0.040	0.500	0.261	0.239	200.	211.	17872.	124.
ITL-18	3P5601	482.	0.400	0.500	0.251	0.249	208.	209.	36295.	25.
ITL-17	3P5601	538.	0.040	0.500	0.257	0.243	199.	197.	15165.	105.
ITL-8	3P5601	538.	0.400	0.970	0.274	0.699	238.	239.	2000.	3.
ITL-15	3P5601	538.	0.400	0.720	0.260	0.460	217.	240.	4376.	15.
ITL-12	3P5601	538.	0.400	0.710	0.270	0.440	233.	226.	2758.	48.
ITL-68	3P5601	538.	0.400	0.700	0.240	0.460	214.	207.	2974.	51.
ITL-17	3P5601	538.	0.400	0.560	0.240	0.320	221.	207.	2593.	59.
ITL-40	3P5601	538.	0.400	0.503	0.263	0.240	237.	224.	15765.	11.
AP12	3P5601	538.	0.400	0.500	0.212	0.288	184.	186.	19809.	14.

(NEXT PAGE)

ORNL CONTINUOUS CYCLING FATIGUE DATA FOR 2.25CR-1-Mn STEEL
 STRAIN CONTROLLED
 (CONTINUED)

SPECIMEN NUMBER	HEAT NUMBER	TEMP °F	STRAIN RATE (1/SEC.)	STRAIN RANGE (%)	ELASTIC STRAIN AT NF/2 (%)	PLASTIC STRAIN RANGE AT NF/2 (%)	TENSILE STRENGTH AT NF/2 (MPA)	COMPRESSIVE STRESS AMPLITUDE AT NF/2 (MPA)	CYCLES TO FAILURE (NF)	TIME TO FAILURE (HRS)
IUL-6	3P5601	538.	0.400	0.500	0.236	0.264	204.	208.	1074.	7.
AP07	3P5601	538.	0.400	1.000	0.254	0.746	219.	224.	2495.	3.
ITL-18	3P5601	538.	0.400	1.000	0.280	0.720	252.	243.	1527.	15.
ITL-75	3P5601	538.	0.400	1.010	0.270	0.740	234.	228.	37.	
ITL-100	3P5601	538.	0.400	1.020	0.290	0.730	241.	271.	1480.	8.
IUL-1G	3P5601	538.	0.400	1.996	0.320	1.676	274.	284.	679.	2.
AP03	3P5601	538.	0.400	2.000	0.294	1.706	254.	259.	754.	2.
ITL-61	3P5601	538.	0.400	2.000	0.310	1.690	241.	303.	532.	172.
ITL-11	3P5601	538.	0.400	2.000	0.310	1.690	288.	243.	496.	227.
ITL-22	3P5601	538.	0.400	2.060	0.280	2.680	252.	245.	315.	240.
ITL-20	3P5601	538.	0.400	2.980	0.350	2.630	253.	346.	147.	135.
ITL-62	3P5601	538.	0.400	2.980	0.320	2.660	319.	248.	293.	274.
AP11	3P5601	538.	0.400	0.320	0.350	0.225	0.125	197.	196.	272940.
IUL-7	3P5601	538.	0.400	0.381	0.227	0.144	209.	205.	73256.	34.
ITL-7	3P5601	538.	0.400	0.420	0.206	0.214	179.	179.	63906.	31.
AP16	3P5601	538.	0.400	0.500	0.211	0.255	182.	186.	41500.	23.
ITL31A	3P5601	593.	0.400	0.502	0.227	0.107	161.	178.	8437.	59.
ITL-31	3P5601	593.	0.400	0.500	0.244	0.255	182.	186.	17254.	12.
ITL-34	3P5601	593.	0.400	0.500	0.393	0.107	188.	166.	4200.	292.
LC-20	50557	93.	0.400	0.502	0.213	0.290	206.	206.	32800.	23.
LC-11	50557	316.	0.400	0.500	0.226	0.274	198.	211.	38126.	25.
LC-16	50557	371.	0.400	0.500	0.200	0.300	209.	222.	21061.	15.
LC-9	50557	427.	0.400	0.505	0.256	0.249	193.	198.	13895.	97.

[NEXT PAGE]

MRNL CONTINUOUS CYCLING FATIGUE DATA FRP 2-25CR-1-MG STEEL
 STRAIN CONTROLLED
 (CONTINUOUS)

SPECIMEN NUMBER	HEAT NUMBER	TEMP DEG C	STRAIN RATE 1/sec	ELASTIC STRAIN (%)	PLASTIC STRAIN RANGE AT NF/2 (%)	TENSILE STRESS AMPLITUDE AT NF/2 (MPA)	CYCLES TO FAILURE IN	TIME TO FAILURE (HRS)
LC-19	50557	427.	0.400	1.002	0.273	0.720	249.	2709.
LC-7	50557	427.	0.400	1.010	0.293	0.717	265.	2612.
LC-18	50557	427.	0.400	2.000	0.311	1.689	270.	286.
LC-17	50557	427.	0.400	3.006	0.373	2.633	302.	313.
LC-15	50557	427.	0.400	0.350	0.232	0.118	200.	211.
LC-12	50557	427.	0.400	0.398	0.240	0.158	197.	210.
LC-6	50557	538.	0.400	0.902	0.295	0.697	216.	222.
LC-3	50557	538.	0.400	0.688	0.260	0.428	203.	212.
LC-2	50557	538.	0.400	0.500	0.288	0.211	183.	185.
LC-4	50557	538.	0.400	2.019	0.331	1.688	235.	244.
LC-8	50557	538.	0.400	0.364	0.170	0.134	142.	154.
LC-5	50557	538.	0.400	0.400	0.203	0.197	177.	178.
LC-5	50557	538.	0.400	0.401	0.225	0.176	177.	185.
LC-21	50557	593.	0.400	0.500	0.192	0.208	176.	183.
VPH01	56447	427.	0.400	0.500	0.249	0.251	228.	231.
VIL-22	56447	427.	0.400	0.500	0.329	0.171	300.	303.
VPU12	56447	427.	0.400	0.250	0.215	0.035	100.	186.
VPH06	56447	427.	0.400	1.000	0.293	0.707	269.	272.
VPH09	56447	427.	0.400	2.000	0.344	1.656	317.	317.
VPH04	56447	427.	0.400	0.300	0.204	0.096	193.	193.
VPH08	56447	427.	0.400	0.400	0.236	0.164	214.	221.
VIL-24	56447	427.	0.400	0.400	0.276	0.124	248.	260.
VPH12	56447	538.	0.400	0.530	0.208	0.312	179.	183.

(NEXT PAGE)

NON-CONTINUOUS CYCLING FATIGUE DATA FOR 2.25CR-1.4N STEEL
STRAIN CONTROLLED
(CONTINUENT)

SPECIMEN	HEAT NUMBER	TEMP DFG C	STRAIN RATE (#/SEC)	STRAIN RANGE (%)	PLASTIC STRAIN (%)	PLASTIC STRESS RANGE (MPA)	TENSILE STRESS AMPLITUDE AT NF/2 (%)	COMPRESSIVE STRESS AMPLITUDE AT NF/2 (%)	CYCLES TO FAILURE (NF)	TIME TO FAILURE (HRS)
VIL-25	56447	538.	0.400	0.500	0.279	0.221	241.	245.	29825.	21.
VPU07	56447	538.	0.400	0.250	0.167	0.383	147.	145.	50107.	174.
VPH14	56447	538.	0.400	1.000	0.259	0.741	224.	228.	2160.	3.
VPH13	56447	538.	0.400	2.000	0.292	1.708	250.	260.	488.	7.
VPH16	56447	538.	0.400	0.300	0.189	0.111	159.	170.	586419.	243.
VPH15	56447	538.	0.400	0.400	0.192	0.208	165.	169.	71417.	40.
VIL-27	56447	538.	0.400	0.400	0.262	0.138	275.	231.	38927.	27.

TRUL FATIGUE DATA FOR 2.25Cr-1.0Mo STEEL
STRAIN CONTROLLED

SPECIMEN NUMBER	TEMP DEG C	STRAIN RATE 1/S	FREQUENCY (HZ)	HOLD TIME (HRS)	HOLD MODE	PLASTIC STRAIN RANGE AT NF/2		TENSILE STRESS RANGE AT NF/2		COPPERSTIF STRESS AMPLITUDE 14PA		CYCLES TO FAILURE (HRS)	TIME TO FAILURE (HRS)
						1/S	(%)	14PA	14PA	14PA	14PA		
I6012	538.	3.089	0.400	0.0670	0.500	COMPRESSION	2.688	0.375	324.	329.	191.	306.	155.
I6017	593.	3.015	0.400	0.3670	0.500	COMPRESSION	2.638	0.377	317.	319.	218.	296.	
ITL-30	482.	0.500	0.400	0.0028	0.050	33TH	0.276	0.224	172.	176.	131.	352.	355.
ITL-106	482.	0.500	0.400	0.0028	0.100	TENSION	0.252	0.248	230.	236.	157.	15450.	1556.
ITL-15	538.	0.500	0.400	0.3260	0.010	COMPRESSION	0.266	0.236	187.	180.	155.	8251.	89.
ITL-46	538.	0.500	0.400	0.3260	0.010	TENSION	0.280	0.220	184.	213.	148.	22986.	246.
ITL-67	538.	2.990	0.400	0.3670	0.500	COMPRESSION	2.619	0.377	323.	335.	175.	310.	156.
ITL-44	593.	0.500	0.400	0.3260	0.010	TENSION	0.250	0.250	196.	230.	152.	17780.	190.
ITL-60	593.	3.060	0.400	0.0670	0.500	COMPRESSION	2.700	0.350	291.	298.	209.	335.	169.
ITL-39	593.	0.499	0.400	0.3260	0.010	COMPRESSION	0.301	0.198	178.	176.	133.	6420.	69.

Appendix B

Figs. AB-1 to AB-7 are
Representative Cyclic Creep Curves
Generated on 2 1/4 Cr-1 Mo Steel

(Predicted lines shown were calculated
from the creep equation in Ref. 9
assuming identical behavior in tension
and compression.)

ORNL-DWG 76-15226R

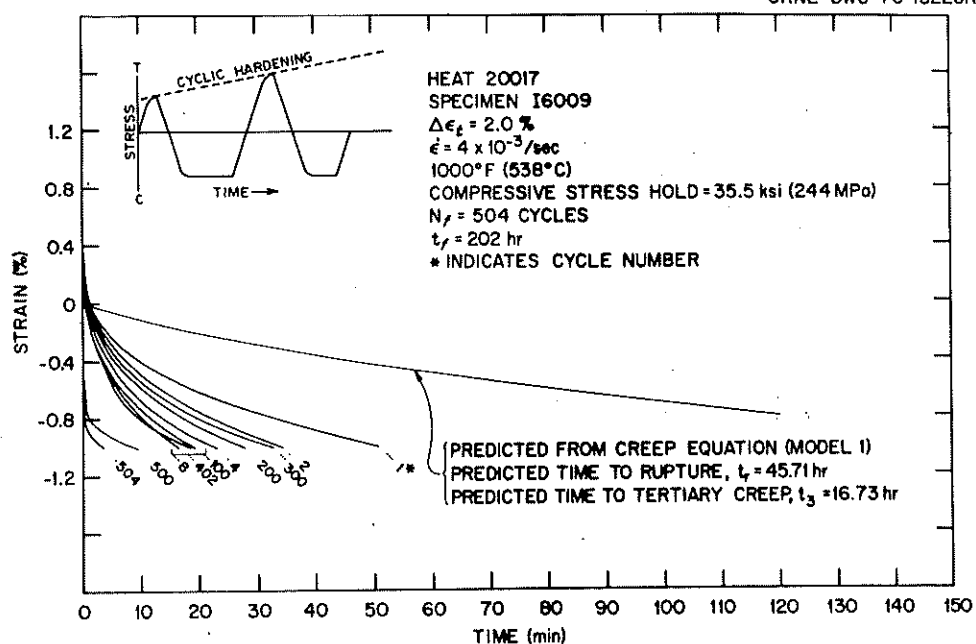


Fig. AB-1. Creep Strain vs Time During a Creep-Fatigue Test with a Compressive Stress Hold Period for 2 1/4 Cr-1 Mo Steel, Heat 20017, Tested at 1000°F (538°C).

ORNL-DWG 76-16480R

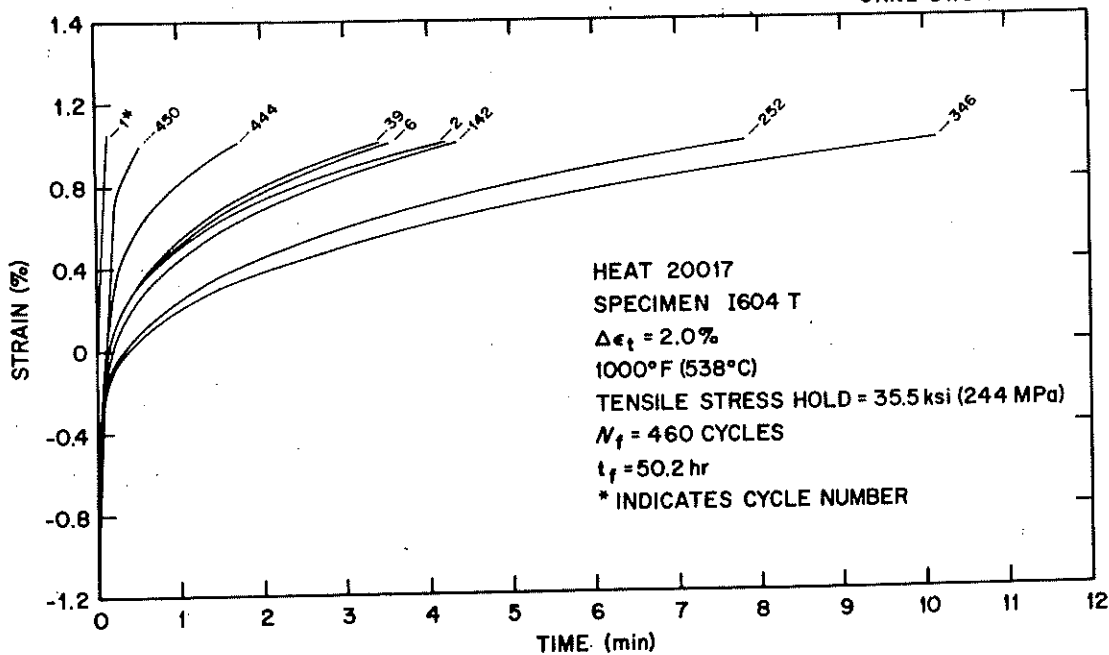


Fig. AB-2. Creep Strain vs Time During a Creep-Fatigue Test with a Tensile Stress Hold Period for 2 1/4 Cr-1 Mo Steel, Heat 20017, Tested at 1000°F (538°C).

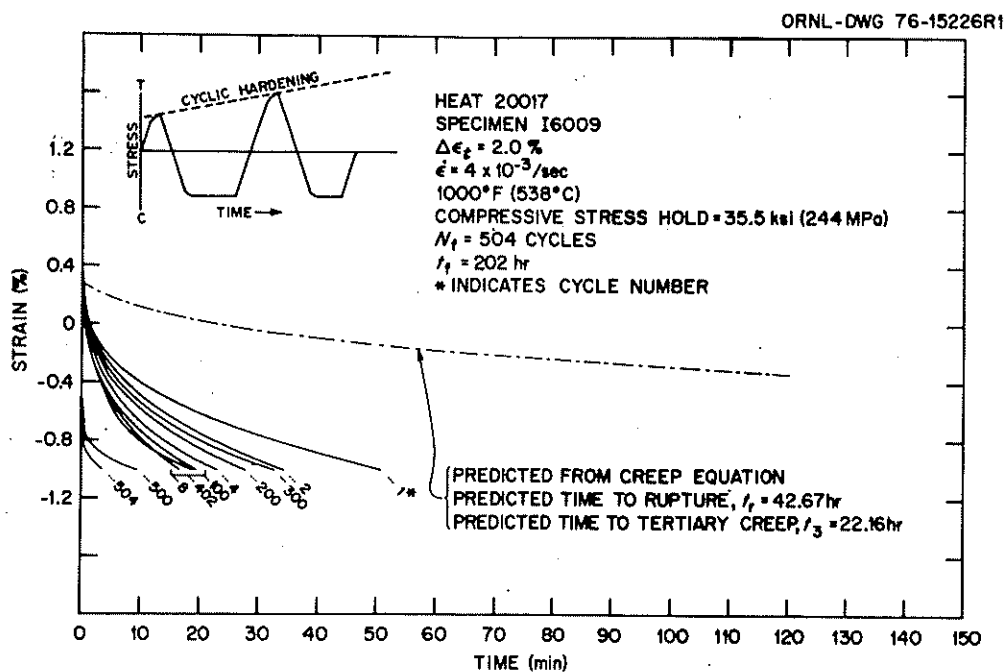


Fig. AB-3. Creep Strain vs Time During a Creep-Fatigue Test with a Compressive Stress Hold Period for 2 1/4 Cr-1 Mo Steel, Heat 20017, Tested at 1000°F (538°C).

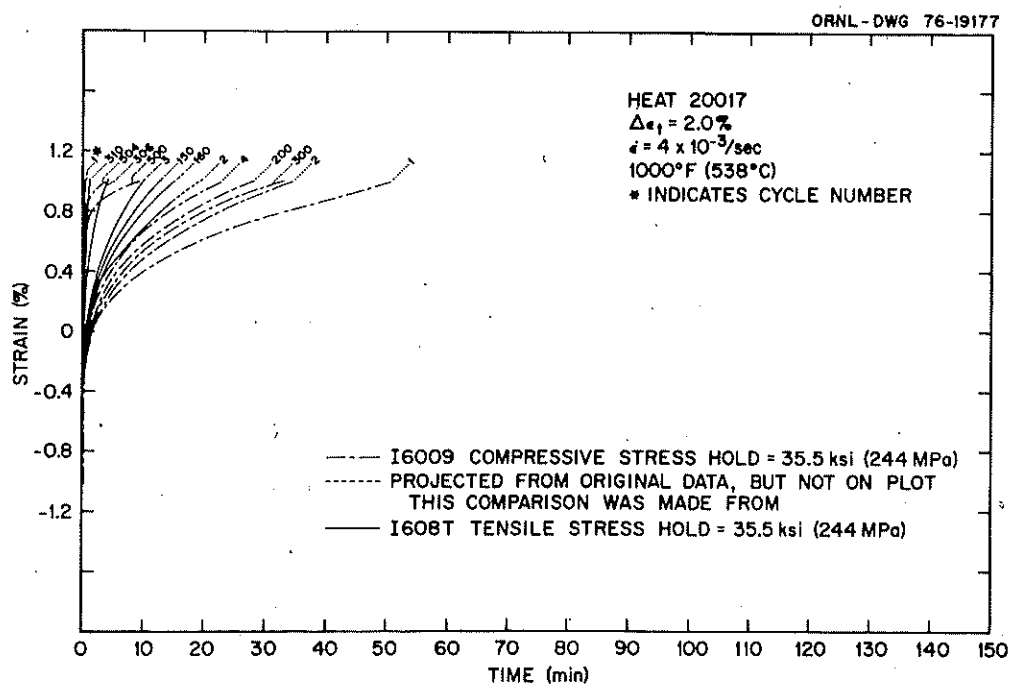
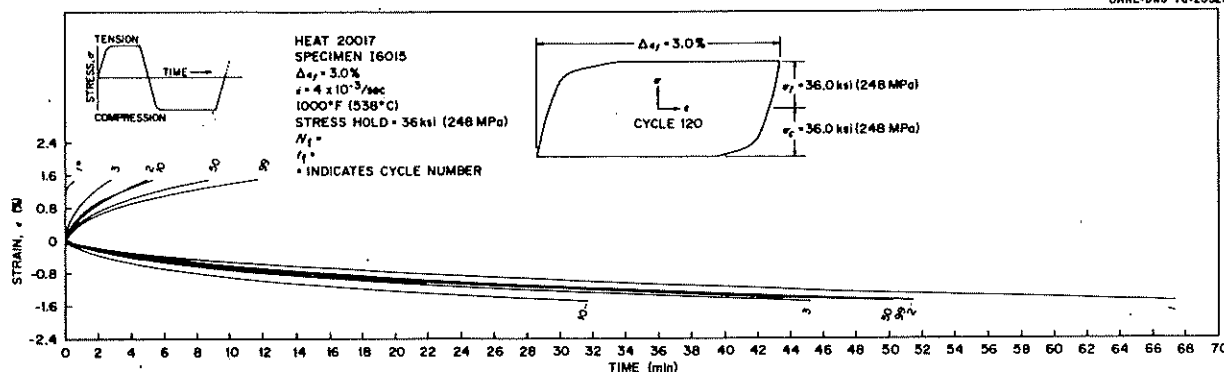
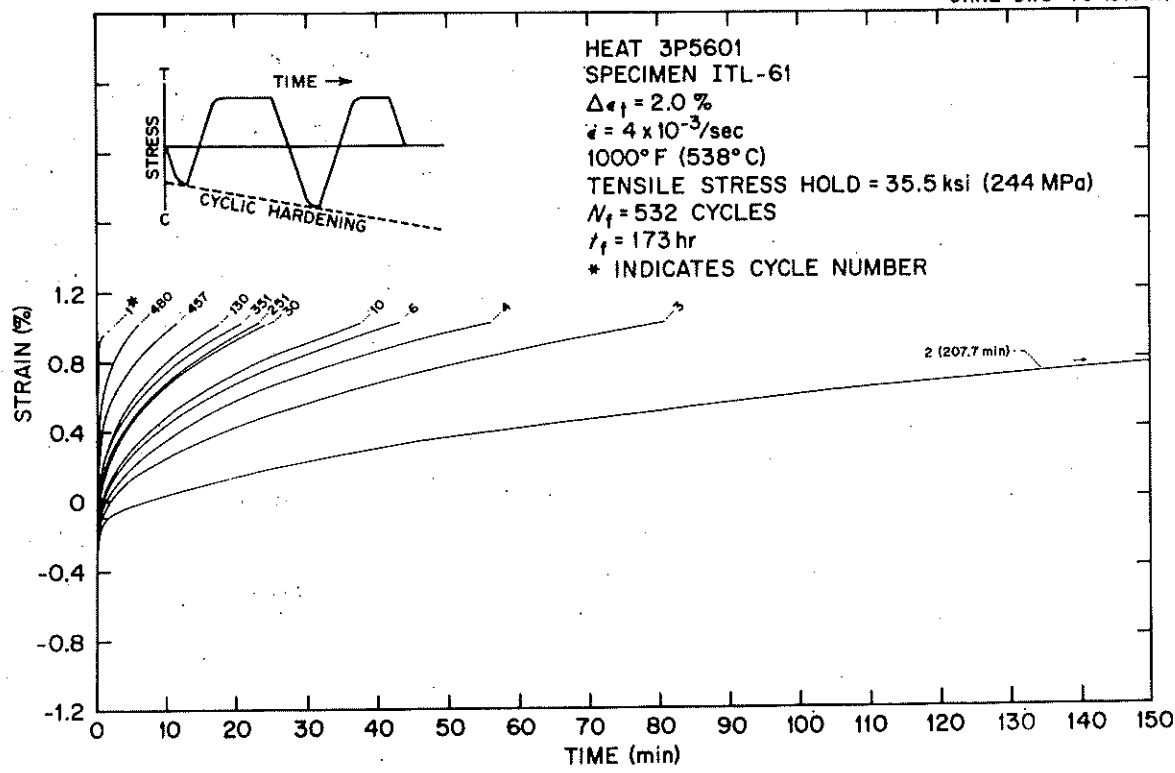


Fig. AB-4. Comparisons Between Cyclic Creep Curves Generated for Either a Tensile "cp" or Compressive "pc" Load Hold at the Same Stress Level. Note the tendency for a higher tensile creep rate.

ORNL-DWG 76-20521



ORNL-DWG 76-19174R



ORNL-DWG 76-15227R

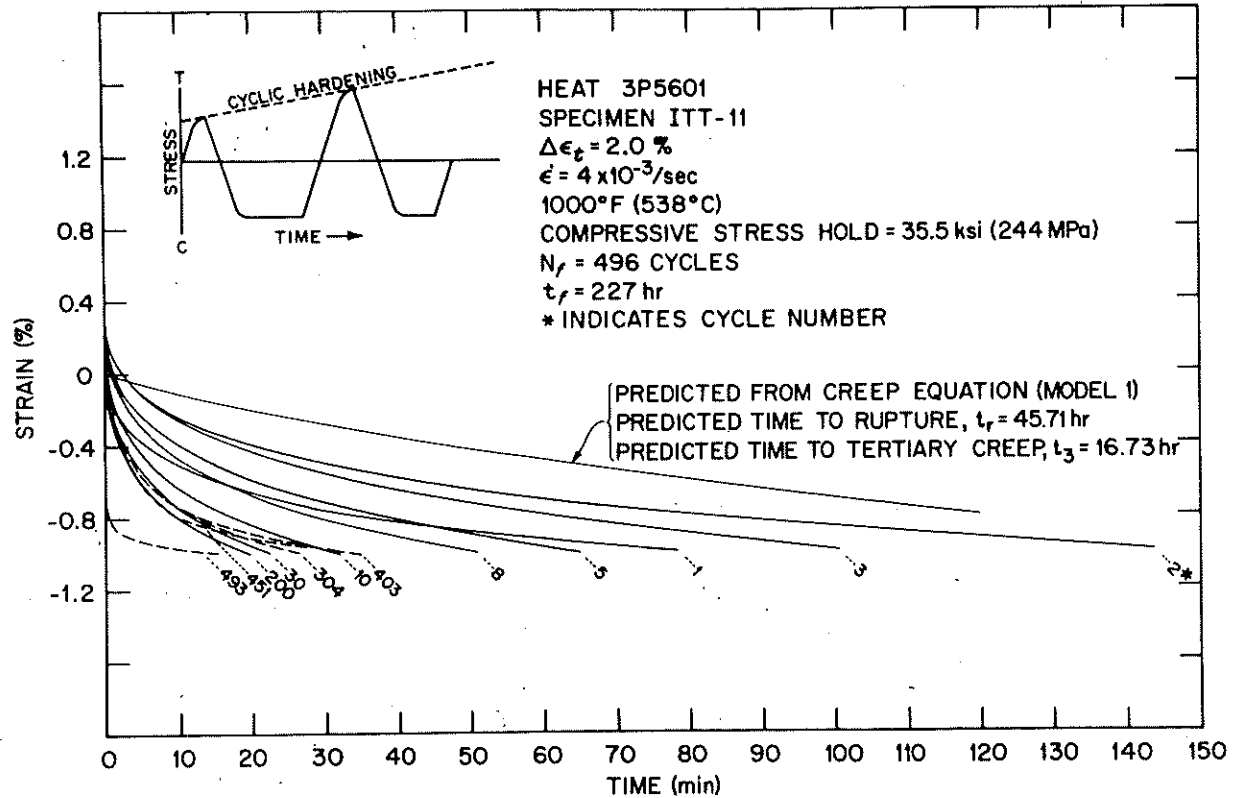


Fig. AB-7. Creep Strain vs Time During a Creep Fatigue Test with a Compressive Stress Hold Period for 2 1/4 Cr-1 Mo Steel, Heat 3P5601. Tested at 1000°F (538°C).

Appendix C

Tables AC-1 to AC-10 contain the results of calculations obtained using concepts of strain-range partitioning. Tables AC-1 to AC-6 contain calculations for 2 1/4 Cr-1 Mo steel, Table AC-7 contains calculations for Hastelloy X, and Tables AC-8 to AC-10 contain calculations for Type 316 stainless steel.

Table AC-1. Predicted Strain Components and Cycles to Failure
 2 1/4 Cr-1 Mo Steel at 482°C Calculated From
 $\ln(\sigma_0/\sigma) = C_{t0} \cdot 14\alpha$

Hold Period (hr)	$\Delta\sigma/2$ (MPa)	Partitioned Strain Components (%)			Predicted Cyclic Lifetimes, Cycles		
		$\Delta\varepsilon_{pc}$		$\Delta\varepsilon_{in}$	Compressive Hold	Tensile Hold	
		$\Delta\varepsilon_{pp}$	$\Delta\varepsilon_{cp}$				
<u>Total Strain Range 0.4%, C = 0.30</u>							
0	—	—	—	—	53,835 ^b	53,835 ^b	
0.01	215	0.141	0.0195	0.160	289,868 ^c	289,868 ^c	
0.1	194	0.171	0.0231	0.194	17,509	31,918	
100	183	0.183	0.0447	0.228	13,410	21,347	
					7,455	11,643	
<u>Total Strain Range 0.5%, C = 0.30</u>							
0	—	—	—	—	36,784 ^d	36,784 ^d	
0.01	227	0.231	0.0207	0.252	10,745	13,800	
0.1	207	0.255	0.0248	0.280	8,534	10,537	
100	202	0.261	0.0526	0.314	5,050	6,373	
<u>Total Strain Range 1.0%, C = 0.47</u>							
0	—	—	—	—	—	—	2,942 ^d
0.01	312	0.361	0.0408	0.672	2,220	2,149	
0.1	285	0.660	0.0491	0.712	2,026	1,933	
100	265	0.686	0.0934	0.780	1,588	1,440	

(continued)

Table AC-1 (continued)

Hold Period (hr)	$\Delta\sigma/2$ (MPa)	Partitioned Strain Components (%)		Predicted Cyclic Lifetimes, Cycles
		$\Delta\varepsilon_{pc}$	$\Delta\varepsilon_{cp}$	
<u>Total Strain Range 2.0, C = 0.47</u>				
0	—	—	—	910 ^d
0.01	350	1.58	0.046	746
0.1	315	1.63	0.054	832
100	300	1.739	0.105	696
				664
				531

^aCreep component may be $\Delta\varepsilon_{pc}$ or $\Delta\varepsilon_{cp}$

^bHeat 20017

^cHeat 3P5601

^dAverage value

^eStatic Young's Modulus = 1.69×10^5 MPa

Table AC-2. Predicted Strain Components and Cycles to Failure
 for Annealed 2 1/4 Cr-1 Mo Steel at 482°C Calculated from
 $\zeta_n(\sigma_0/\sigma) = Ct^{0.14}$ and Assuming a Relaxed Stress Range
 of $1.2\Delta\sigma_r$

Hold Period (hr)	$\Delta\sigma/2$ (MPa)	Partitioned Strain Components (%)			Predicted Cyclic Lifetimes, Cycles		
		$\Delta\epsilon_{pp}$	$\Delta\epsilon_{p\bar{a},e}$	$\Delta\epsilon_{inf}$	Compressive Hold	Tensile Hold	
<u>Total Strain Range 0.4%, $C = 0.30$</u>							
0	-	-	-	-	53,835 ^b	53,835 ^b	
0.01	215	0.160	0.022	0.181	289,868 ^c	289,868 ^c	
0.1	194	0.183	0.026	0.209	14,653	24,499	
100	183	0.196	0.054	0.249	11,617	17,774	
					6,105	9,134	
<u>Total Strain Range 0.5%, $C = 0.30$</u>							
0	-	-	-	-	36,784 ^d	36,784 ^d	
0.01	227	0.247	0.023	0.270	9,293	11,607	
0.1	207	0.269	0.028	0.297	7,428	9,003	
100	202	0.273	0.060	0.334	4,388	5,404	
<u>Total Strain Range 0.1%, $C = 0.47$</u>							
0	-	-	-	-	2,942 ^d	2,942 ^d	
0.01	312	0.651	0.046	0.697	2,090	2,004	
0.1	285	0.681	0.056	0.737	1,901	1,793	
100	265	0.705	0.105	0.810	1,482	1,321	

(continued)

Table AC-2 (continued)

Hold Period (hr)	$\Delta\sigma/2$ (MPa)	Partitioned Strain Components (%)		Predicted Cyclic Lifetimes, Cycles	
		$\Delta\varepsilon_{pp}^a, e$	$\Delta\varepsilon_{in}^f$	Compressive Hold	Tensile Hold
		Total Strain Range 2.0%, $C = 0.47$			
0	—	—	—	—	—
0.01	350	1.617	0.043	1.660	910d
0.1	315	1.658	0.051	1.709	817
100	300	1.665	0.118	1.783	781
				675	692
					531

^aCreep component may be $\Delta\varepsilon_{pc}$ or $\Delta\varepsilon_{cp}$ ^bHeat 20017^cHeat 3P601^dAverage value^eDynamic Young's Modulus = 1.79×10^5 MPa^f $\Delta\varepsilon_{in} = \Delta\varepsilon_t - (\Delta\sigma - 1.2\Delta\sigma_r)/E$

Table AC-3. Predicted Strain Components and Cycles to Failure for Annealed 2 1/4 Cr-1 Mo Steel at 482°C Calculated $\ln(\sigma_0/\sigma) = Ct^0 \cdot 1^4$

Hold Period (hr)	$\Delta\sigma/2$ (MPa)	Relaxation = $\Delta\sigma_r$				Relaxation = $1.2\Delta\sigma_r$			
		Partitioned Strain Components (%)		Predicted Cyclic Lifetime, Cycles		Partitioned Strain Components (%)		Predicted Cyclic Lifetime, Cycles	
		$\Delta\varepsilon_{pp}$	$\Delta\varepsilon_{in}^b$	$\Delta\varepsilon_{cc}$	$\Delta\varepsilon_{in}^b$	$\Delta\varepsilon_{pp}$	$\Delta\varepsilon_{cc}$	$\Delta\varepsilon_{in}^c$	$\Delta\varepsilon_{in}^c$
Total Strain Range 0.35%, C = 0.30									
0	—	—	—	—	825,234 ^a	—	—	—	825,234 ^a
0.01	210	0.132	0.0173	0.149	28,862	0.136	0.0207	0.157	24,355
0.1	189	0.159	0.0211	0.181	19,787	0.164	0.0254	0.190	17,490
100	178	0.195	0.0435	0.238	9,816	0.203	0.0522	0.256	8,139
Total Strain Range 0.50%, C = 0.30									
0	—	—	—	—	36,784 ^a	—	—	—	36,784 ^a
0.01	227	0.266	0.0195	0.285	10,580	0.269	0.023	0.290	9,908
0.1	207	0.292	0.0234	0.316	8,269	0.297	0.028	0.325	7,445
100	202	0.324	0.0497	0.374	4,837	0.334	0.060	0.394	4,151
Total Strain Range 2.0%, C = 0.47									
0	—	—	—	—	910 ^a	—	—	—	910 ^a
0.01	350	1.65	0.043	1.69	805	1.660	0.052	1.713	784
0.1	315	1.70	0.051	1.75	765	1.709	0.061	1.770	745
100	300	1.76	0.099	1.86	670	1.780	0.118	1.900	641

^aAverage cycles to failure from two tests,

^b $\Delta\varepsilon_{in} = \Delta\varepsilon_t - (\Delta\sigma - 2\Delta\sigma_r)/E$

^c $\Delta\varepsilon_{in} = \Delta\varepsilon_t - (\Delta\sigma - 2.4\Delta\sigma_r)/E$ E = Dynamic Young's Modulus = 1.79×10^5 MPa

Table AC-4. Predicted Strain Components and Cycles to Failure
 for Annealed 2 1/4 Cr-1 Mo Steel at 538°C.
 Stress Levels Were Calculated Using the
 Creep Equation.

Hold Period (hr)	$\Delta\sigma/2$ (MPa)	Relaxed Stress (MPa)	Type II Creep			Type I Creep						
			Partitioned Strain Components (%)			Predicted Cyclic Lifetimes, Cycles						
			$\Delta\varepsilon_{pc}^a$	$\Delta\varepsilon_{pp}$ or $\Delta\varepsilon_{in}$	$\Delta\varepsilon_{cp}$	Compressive Hold	Tensile Hold	Relaxed Stress (MPa)	$\Delta\varepsilon_{pp}$ or $\Delta\varepsilon_{in}$	Compressive Hold	Tensile Hold	
Total Strain Range 0.25%												
0	—	—	—	—	—	3,787,765 ^b	3,787,765 ^b	—	—	—	3,787,765 ^b	3,787,765 ^b
0.01	172	170	0.028	0.001	0.029	461,487 ^d	—	170	0.028	0.001	461,487 ^d	461,487 ^d
0.1	162	151	0.041	0.007	0.048	65,996 ^d	—	152	0.041	0.007	65,996 ^d	65,996 ^d
100	148	61	0.059	0.056	0.115	7,830 ^d	—	77	0.059	0.046	105	9,580 ^d
Total Strain Range 0.30%												
0	—	—	—	—	—	408,424 ^c	408,424 ^c	—	—	—	408,424 ^c	408,424 ^c
0.01	177	174	0.072	0.002	0.074	163,815 ^d	—	174	0.072	0.002	163,815 ^d	163,815 ^d
0.1	167	154	0.085	0.008	0.093	48,456 ^d	—	155	0.085	0.007	54,416 ^d	54,416 ^d
100	155	61	0.100	0.061	0.161	6,751 ^d	—	77	0.10	0.050	150	8,232 ^d
Total Strain Range 0.40%												
0	—	—	—	—	—	48,595 ^c	48,595 ^c	—	—	—	48,595 ^c	48,595 ^c
0.01	188	183	0.157	0.003	0.161	47,363 ^d	—	184	0.157	0.003	160	47,704 ^d
0.1	180	160	0.168	0.013	0.181	20,641 ^d	—	161	0.167	0.012	180	21,806 ^d
100	160	62	0.194	0.0632	0.257	5,337 ^d	—	79	0.194	0.052	246	6,330 ^d

(continued)

Table AC-4 (continued)

Hold Period (hr)	$\Delta\sigma/2$ (MPa)	Relaxed Stress (MPa)	Type II Creep				Type I Creep			
			Partitioned Strain Components (%)		Predicted Cyclic Lifetimes, Cycles		Partitioned Strain Components (%)		Predicted Cyclic Lifetimes, Cycles	
			$\Delta\varepsilon_{pc}^a$	$\Delta\varepsilon_{pp}$ or $\Delta\varepsilon_{in}$	Compressive Hold	Tensile Hold	Relaxed Stress (MPa)	$\Delta\varepsilon_{pp}$ or $\Delta\varepsilon_{ep}$	Compressive Hold	Tensile Hold
Total Strain Range 0.50%										
0	—	—	—	—	16,161c	16,161c	—	—	—	16,161c
0.01	203	194	0.238	0.006	0.244	17,418	19,504	0.238	0.004	19,186
0.1	195	165	0.248	0.019	0.267	10,272	12,590	0.248	0.017	10,875
100	177	62	0.271	0.074	0.345	3,761	4,633	0.272	0.063	4,259
Total Strain Range 1.0%										
0	—	—	—	—	—	2,513	2,513	—	—	2,513
0.01	242	211	0.688	0.020	0.708	2,299	2,250	0.687	0.010	0.698
0.1	235	169	0.697	0.043	0.739	1,990	1,898	180	0.036	0.732
100	220	64	0.798	0.101	0.899	1,366	1,194	82	0.716	0.089
Total Strain Range 2.0%										
0	—	—	—	—	—	839c	839c	—	—	839c
0.01	287	216	1.632	0.046	1.678	803	719	250	1.629	0.024
0.1	281	171	1.637	0.071	1.708	757	645	188	1.637	0.060
100	269	66	1.652	0.131	1.783	664	512	84	1.653	0.119

^aStatic Young's Modulus Employed 1.55×10^5 MPa, ^bSpecimen Did Not Fail After 1,710,960 Cycles, Cyclic Life Estimated From Fatigue Equation

^cAverage Values,
^dValues Not Calculated

Table AC-5. Predicted Strain Components and Cycles to Failure
for Annealed 2 1/4 Cr-1 Mo Steel at 538°C Calculated from
 $\ln(\sigma_0/\sigma) = Ct^{0.14}$ or the ORNL Creep Equation

Relaxation Behavior Predicted by the Gittus Equation						Relaxation Behavior Predicted by the Creep Equation					
Hold Period (hr)	$\Delta\sigma/2$ (MPa)	Partitioned Strain Components (%)			σ_r (MPa)	$\sigma_r/2$ (MPa)	Type I Creep			Type II Creep	
		$\Delta\epsilon_{pp}$	$\Delta\epsilon_{cc}$	$\Delta\epsilon_{in}^a$			$\Delta\epsilon_{pp}$	$\Delta\epsilon_{cc}$	$\Delta\epsilon_{in}$	$\Delta\epsilon_{pp}$	$\Delta\epsilon_{cc}$
Total Strain Range 0.5%, $C = 0.55$						Total Strain Range 0.5%					
0	—	—	—	—	16,161 ^b	—	—	—	—	16,161 ^b	—
0.01	212	0.288	0.030	0.318	7,590	203	197	194	0.272	0.003	0.275
0.1	203	0.305	0.037	0.342	6,230	195	168	165	0.293	0.015	0.308
100	191	0.357	0.075	0.432	3,293	177	80	62	0.354	0.055	0.409
Total Strain Range 1.0%, $C = 0.80$						Total Strain Range 1.0%					
0	—	—	—	—	2,513 ^b	—	—	—	—	2,513 ^b	—
0.01	260	0.753	0.051	0.805	1,853	242	226	211	0.733	0.009	0.742
0.1	249	0.779	0.062	0.841	1,713	235	180	169	0.763	0.031	0.794
100	234	0.837	0.105	0.942	1,374	220	82	64	0.827	0.079	0.906
Total Strain Range 2.0%, $C = 0.80$						Total Strain Range 2.0%					
0	—	—	—	—	839 ^b	—	—	—	—	839 ^b	—
0.01	300	1.716	0.058	1.774	746	287	250	216	1.693	0.021	1.714
0.1	293	1.738	0.074	1.812	713	281	188	171	1.732	0.053	1.785
100	283	1.804	0.126	1.930	623	269	84	66	1.798	0.106	1.904

^a $\Delta\epsilon_{in} = \Delta\epsilon_t - (\Delta\sigma - 2\Delta\sigma_r)/E$

^bValues for no hold time calculated from average continuous cycling fatigue data

^cDynamic Young's Modulus = 1.75×10^5 MPa

Table AC-6. Long-Hold-Period Strain Components and Creep Fatigue Lives for 2 1/4 Cr-1 Mo Steel at 538°C Calculated
 $\ln(\sigma_0/\sigma) = Ct^{0.14}$

Hold Period (hr)	$\Delta\sigma/2$ (MPa)	Partitioned Strain ^d Components (%)		Predicted Lives, ^b Cycles	
		$\Delta\epsilon_{pp}^a$	$\Delta\epsilon_{pc}^a$	Strain Range Partitioning	
				Tensile Hold	Compressive Hold
<u>Total Strain Range 0.4%, C = 0.55</u>					
0	—	—	—	48,595 ^c	48,595 ^c
0.01	202	0.027	0.027	e	12,420
0.1	188	0.185	0.034	e	9,320
1	182	0.192	0.044	e	7,349
10	178	0.196	0.056	e	5,904
100	174	0.201	0.068	e	4,909
<u>Total Strain Range 0.5%, C = 0.55</u>					
0	—	—	—	16,161	16,161
0.1	203	0.268	0.037	7,754	6,289
1	198	0.274	0.048	6,333	5,151
10	194	0.279	0.061	5,192	4,257
100	191	0.282	0.075	4,349	3,601
<u>Total Strain Range 0.25%, C = 0.3</u>					
0	—	—	—	3,787,765	3,787,765
0.01	154	0.074	0.009	e	45,845
0.1	158	0.075	0.017	e	25,035
100	147	0.082	0.039	e	10,895
<u>Total Strain Range 1.0%, C = 0.80</u>					
0	—	—	—	2,513	2,513
0.1	249	0.716	0.060	1,660	1,781
1	241	0.724	0.076	1,498	1,639
10	238	0.728	0.093	1,361	1,517
100	234	0.732	0.109	1,250	1,418
<u>Total Strain Range 2.0%, C = 0.80</u>					
0	—	—	—	839	839
0.1	293	1.665	0.071	633	744
1	289	1.670	0.091	587	711
10	288	1.671	0.113	538	680
100	283	1.676	0.131	504	655

^a"Creep" component may be $\Delta\epsilon_{pp}$ or $\Delta\epsilon_{cp}$.

^bValues for no hold time calculated from average values of continuous cycling fatigue data.

^cValue for no hold time calculated from best fits to continuous cycling fatigue data.

^dDynamic Young's Modulus = 1.75×10^5 MPa

^eValues not calculated

Table AC-7. Comparison of Actual and Predicted Cyclic Life for Hastelloy X (Heat 2600-3-34936, 13-mm plate) Tests in Air in Strain Control

Test Temperature (°C)	Specimen Number	Total Strain Range, %	Inelastic Strain Range ^a Components, %				Cyclic Life, Cycles			Duration of Hold Period, hr	Time to Failure, hr
			$\Delta\epsilon_{in}^a$	$\Delta\epsilon_{cp}$	$\Delta\epsilon_{pc}$	$\Delta\epsilon_{pp}$	$\Delta\epsilon_{cc}$	Actual Predicted			
								Cyclic	Cyclic Life		
871	HXL-33	2.01	1.550	—	—	1.550	—	312	211	0	0.9
871	HXL-34	2.0	1.732	0.200	—	1.532	—	216	141	0.1(T)	22.2
871	HXL-35	2.0	1.729	—	0.210	1.519	—	185	188	0.1(C)	19.0
871	HXL-37	2.0	1.952	—	0.004	1.738	0.210	196	130	0.1(T+C)	39.8
871	HXL-21	0.59	0.260	—	—	0.26	—	3,433	3,371	0	2.9
871	HXL-26	0.6	0.347	0.110	—	0.237	—	2,191	1,408	0.1(T)	219.9
871	HXL-32	0.6	0.364	—	0.140	0.224	—	1,084	2,494	0.1(C)	108.8
871	HXL-38	2.0	0.559	—	—	0.399	0.160	984	807	0.1(T+C)	197.0
704	HXL-201	1.0	1.170	—	—	1.170	—	415	327	0	0.6
704	HXL-202	1.0	0.427	—	—	0.427	—	1,528	1,561	0	1.0
704	HXL-89	1.0	0.354	—	—	0.354	—	1,570	2,088	0	1.1
704	HXL-81	2.0	1.399	—	0.216	1.183	—	176	126	0.5(C)	87.0
704	HXL-92	2.0	1.489	0.211	—	1.278	—	102	153	0.5(T)	50.8
704	HXL-82	2.0	1.505	—	0.011	1.262	0.232	150	164	0.5(T+C)	149.4

^aYoung's Modulus, 871°C $E = 137$ GPa, 704°C $E = 150$ GPa, (21.8×10^6 psi)

^bC = compressive hold; T = tension hold

Table AC-8. Comparison of Actual and Predicted Cyclic Lives
for Type 316 Stainless Steel^d Tested at 593°C

Specimen No.	Total Strain (%)	Duration of Tensile Hold Time (hr)	Material Condition	Inelastic Strain Range Components, %			Cyclic Lifetime, Cycles	
				$\Delta\epsilon_{in}^a$	$\Delta\epsilon_{cp}$ or $\Delta\epsilon_{pc}$	$\Delta\epsilon_{pp}$	Actual	Calculated Using $\Delta\epsilon_{pp}$ Values
D-223	2.0	0	Annealed ^a	1.43	0	1.43	547	398
D-213	2.0	0	Annealed ^a	1.42	0	1.42	445	404
D-214	1.0	0	Annealed ^a	0.56	0	0.56	2,213	2,638
D-193	0.5	0	Annealed ^a	0.20	0	0.20	27,898	21,026
D-211	2.0	0.01	Annealed ^a	1.45	0.02	1.43	558	189
D-212	2.0	0.01	Annealed ^a	1.58	0.02	1.56	542	168
D-208	2.0	0.0	Annealed ^a	1.42	0.04	1.38	137	128
D-210	2.0	0.1	Annealed ^a	1.43	0.04	1.39	147	126
D-143	2.0	0	Annealed ^a	1.43	0	1.43	450	398
D-139	2.0	0	Annealed ^a	1.46	0	1.46	406	382
D-74	2.0	0	Annealed ^a	1.42	0	1.42	406	404
D-148	1.0	0	Annealed ^a	0.56	0	0.56	2,040	2,638
D-146	1.02	0	Annealed ^a	0.57	0	0.57	2,241	2,546
D-150	0.5	0	Annealed ^a	0.21	0	0.21	29,822	19,056
D-147	0.5	0	Annealed ^a	0.20	0	0.20	23,850	21,026
D-131	2.0	0.01	Annealed ^a	1.40	0.01	1.39	218	268
D-186	1.98	0.01	Annealed ^a	1.44	0.02	1.42	367	190
D-197	2.0	0.1	Annealed ^a	1.42	0.05	1.37	71	109
D-200	2.0	0.1	Annealed ^a	1.45	0.04	1.41	115	125
D-188	1.99	0.5	Annealed ^a	1.45	0.05	1.40	57	106
D-129	2.0	0.5	Annealed ^a	1.53	0.05	1.48	64	111
D-198	2.0	1.0	Annealed ^a	1.46	0.08	1.38	43	74
D-144	2.0	5.16	Annealed ^a	1.54	0.08	1.46	25	70
D-194	2.0	10.0	Annealed ^a	1.52	0.10	1.42	15	59
D-142	1.0	0.01	Annealed ^a	0.57	0.01	0.56	1,170	920
D-164	1.0	0.1	Annealed ^a	0.58	0.01	0.57	393	901
D-184	1.0	0.1	Annealed ^a	0.58	0.01	0.57	438	901
D-145	0.98	0.5	Annealed ^a	0.58	0.04	0.54	221	311
D-173	1.0	5.0	Annealed ^a	0.57	0.06	0.51	84	219
D-141	0.51	0.01	Annealed ^a	0.17	0.004	0.166	8,400	6,643
D-177	0.50	0.1	Annealed ^a	0.17	0.004	0.166	1,985	6,643
D-300	0.50	0.5	Annealed ^a	0.19	0.018	0.172	1,050	1,640
D-162	0.5	1.0	Annealed ^a	0.19	0.02	0.17	812	1,486
D-184	1.0	0.01 [C] ^e	Annealed ^a	0.57	0.003	0.567	2,134	2,511
D-190	1.0	0.1 [C] ^e	Annealed ^a	0.56	0.017	0.543	1,938	2,440
D-79	2.0	0	Control ^b	1.52	0	1.52	581	461
D-77	2.0	0	Control ^b	1.45	0	1.45	608	519
D-81	1.0	0	Control ^b	0.62	0	0.62	3,266	4,341
D-78	0.51	0	Control ^b	0.23	0	0.23	56,671	51,796
D-88	0.51	0	Control ^b	0.21	0	0.21	42,947	65,023

Table AC-8 (continued)

Specimen No.	Total Strain (%)	Duration of Tensile Hold Time (hr)	Material Condition	Inelastic Strain Range Components, %			Cyclic Lifetime, Cycles	
				$\Delta\epsilon_{in}^d$	$\frac{\Delta\epsilon_{cp}}{\Delta\epsilon_{pc}}$	$\Delta\epsilon_{pp}$	Actual	Calculated Using Actual $\Delta\epsilon_{pp}$ Values
D-83	1.99	0.01	Control ^b	1.45	0.02	1.43	658	215
D-85	2.0	0.1	Control ^b	1.48	0.03	1.45	203	162
D-86	2.0	0.5	Control ^b	1.48	0.07	1.41	85	86
D-82	2.0	2.0	Control ^b	1.55	0.06	1.49	146	92
D-226	2.0	0	Control ^c	1.55	0	1.55	914	439
D-221	1.98	0	Control ^c	1.47	0	1.47	534	502
D-215	1.0	0	Control ^c	0.63	0	0.63	2,773	4,171
D-225	0.99	0	Control ^c	0.62	0	0.62	2,603	4,341
D-239	0.78	0	Control ^c	0.47	0	0.47	8,334	8,677
D-216	0.49	0	Control ^c	0.22	0	0.22	106,622	57,884
D-220	2.02	0.01	Control ^c	1.56	0.03	1.53	759	151
D-235	1.98	0.01 [C] ^e	Control ^c	1.534	0.004	1.53	843	450
D-231	1.0	0.01	Control ^c	0.64	0.023	0.617	3,465	502
D-230	4.03	0.1	Control ^c	3.414	0.074	3.34	187	29
D-218	2.0	0.1	Control ^c	1.51	0.03	1.48	608	157
D-234	2.0	0.1	Control ^c	1.49	—	—	650	
D-227	1.0	0.1	Control ^c	0.63	0.03	0.60	2,027	402
D-219	2.0	0.5	Control ^c	1.54	0.04	1.50	446	126

^aSolution Annealed at 1075°C followed by helium quench^bAged 3096 hours at 600°C^cAged 5040 hours at 593°C^dYoung's Modulus, 1.540×10^5 MPa, Heat 65808^e[C] indicates compressive hold time

Table AC-9. Comparison of Actual and Predicted Cyclic Lives
for Type 316 Stainless Steel^c Tested at 565°C

Specimen No.	Total Strain Range (%)	Duration of Tensile Hold Time (hr)	Material Condition	Inelastic Strain Range Components, %			Cyclic Lifetime, Cycles	
				$\Delta\epsilon_{in}^b$	$\Delta\epsilon_{cp}$	$\Delta\epsilon_{pp}^a$	Actual	Calculated Using Actual $\Delta\epsilon_{pp}$ Values
22	1.96	0.1	Annealed	1.50	0.02	1.48	163	176
23	0.97	0.1	Annealed	0.64	0.01	0.63	534	776
68	1.92	1.0	Annealed	1.34	0.02	1.32	76	205
37	2.02	0.1	Aged ^d	1.55	0.03	1.52	197	148
80L	2.08	0.5	Aged ^d	1.54	0.01	1.53	82	268
60	1.00	0.5	Aged ^d	0.57	0.0042	0.566	366	2,200
48	1.88	1.0	Aged ^d	1.44	0.03	1.41	89	163
81L	1.04	1.0	Aged ^d	0.62	0.004	0.616	190	1,845
70	1.90	5.0	Aged ^d	1.38	0.018	1.362	48	240

L = Uniform gage length

^a $\Delta\epsilon_{pp}$ expression from 593°C solution annealed or aged specimen data

^bYoung's Modulus, $E = 1.83 \times 10^6$ MPa

^cHeat B65808

^dAged for 1000 hrs at 565°C prior to test

Table AC-10. Comparison of Actual and Predicted Cyclic Lives
for Irradiated Type 316 Stainless Steel Tested at 593°C

Specimen No.	Total Strain Range (%)	Duration of Tensile Hold Time ^a	Fluence In Units of $10^{26}n/m^2$ $E > 0.1\text{MeV}$	Inelastic Strain Range Components (%)			Cyclic Lifetimes, Cycles	
				$\Delta\varepsilon_{in}^c$	$\Delta\varepsilon_{pe}$ or $\Delta\varepsilon_{cp}$	$\Delta\varepsilon_{pp}^b$	Actual	Calculated Using Actual $\Delta\varepsilon_{pp}$ Values
D-105	2.0	0	2.48	1.38	0	1.38	468	380
D-110	0.98	0	1.98	0.40	0	0.40	942	1,227
D-115	0.50	0	2.10	0.03	0	0.03	15,040	14,318
D-111	2.13	0.01 [C]	1.50	1.48	0.03	1.45	345	326
D-107	0.51	0.01	1.02	0.07	0.009	0.061	4,621	730
D-103	2.0	0.1	2.21	1.40	0.05	1.35	50	17
D-116	1.99	0.1 [C]	1.56	1.41	0.04	1.37	495	332
D-114	1.0	0.1	2.25	0.43	0.02	0.41	88	93
D-106	0.5	0.1	1.85	0.08	0.006	0.074	757	937
D-113	2.0	0.5	1.98	1.39	0.07	1.32	12	12
D-109	1.0	0.5	2.14	0.50	0.02	0.48	60	83
D-108	2.0	5.0	1.90	1.44	0.09	1.35	10	9
D-104	1.0	5.0	2.63	0.52	0.04	0.48	27	42

^a[C] refers to compressive hold time

^bUnirradiated $\Delta\varepsilon_{pp}$ values from 593°C tests conducted on the same heat of material, i.e., Heat 65808

^cYoung's Modulus, $E = 1.540 \times 10^5\text{MPa}$